Warming-driven erosion and sediment transport in cold regions

Ting Zhang[1], Dongfeng Li[1,†], Amy E. East[2], Desmond E. Walling[3], Stuart Lane[4], Irina Overeem[5], Achim A. Beylich[6], Michèle Koppes[7], Xixi Lu[1]

[1] Department of Geography, National University of Singapore, Singapore
[2] U.S. Geological Survey Pacific Coastal and Marine Science Center, Santa Cruz, USA
[3] Department of Geography, College of Life and Environmental Sciences, University of Exeter, Exeter, UK
[4] Institute of Earth Surface Dynamics, University of Lausanne, Lausanne, Switzerland
[5] CSDMS, Institute of Arctic and Alpine Research, University of Colorado Boulder, Boulder, USA
[6] Geomorphological Field Laboratory (GFL), Selbustrand, Norway
[7] Department of Geography, University of British Columbia, Vancouver, Canada

[†]**e-mail**: dongfeng@u.nus.edu

Abstract | Rapid atmospheric warming since the mid-20th century has increased temperature-dependent erosion and sediment transport processes in cold environments, impacting food, energy and water security. In this Review, we summarize landscape changes in cold environments and provide a global inventory of cryosphere degradation-driven increases in erosion and sediment yield. Anthropogenic climate change, deglaciation, and thermokarst disturbances are causing increased sediment mobilization and transport processes in glacierized and peri-glacierized basins. With continuous cryosphere degradation, sediment transport will continue to increase until reaching a maximum (peak sediment). Thereafter, transport will likely shift from a temperature-dependent regime toward a rainfall-dependent regime roughly between 2100-2200. The timing of the regime shift would be regulated by changes in meltwater, erosive rainfall and landscape erodibility, and complicated by geomorphic feedbacks and connectivity. Further progress in integrating multi-source sediment observations, developing physics-based sediment transport models, and enhancing interdisciplinary and international scientific collaboration are needed to predict sediment dynamics in a warming world.

Key points

1. A global inventory of cryosphere degradation-driven increases in erosion and sediment yield is presented, with 76 locations from the high Arctic, European mountains, High Mountain Asia and Andes, and 18 Arctic permafrost-coastal sites.
2. Sediment mobilization from glacierized basins is dominated by glacial and paraglacial erosion; transport efficiency is controlled by glacio-hydrology and modulated by sub-, pro-, supra-glacial storage and release but is interrupted by glacial lakes and moraines.
3. Degraded permafrost mainly mobilizes sediment by eroding thermokarst landscapes in high-latitude terrain and unstable rocky slopes in high-altitude terrain, which is sustained by exposing and melting ground ice and sufficient water supply; transport efficiency is enhanced by hillslope-channel connectivity.
4. The sediment transport regime will shift in three stages, from a thermal-controlled regime to one jointly control by thermal and pluvial processes, and finally to a regime controlled by pluvial processes.
5. Peak sediment yield will be reached with or after peak meltwater.

6. Between the 1950s and 2010s, sediment fluxes have increased by 2-8 folds in many cold regions and coastal erosion rates have more than doubled along many parts of Arctic permafrost coastlines.

[H1] Introduction

Atmospheric warming is driving rapid cryosphere degradation, with increases in temperature-dependent erosion and sediment transport processes in the world's high-altitude and high-latitude cold regions[1,2]. There have been substantial increases in fluvial sediment fluxes from the high Arctic, European mountains, High Mountain Asia (HMA) and the Andes since the 1950s. These hydrogeomorphic changes are dramatically altering terrestrial and coastal landscape evolution, including river and basin reorganization, coastal erosion, and delta progradation[3-5].

Changes in sediment availability and transport capacity[6-8], mobilization[9] and delivery mechanisms have arisen from cryosphere degradation. For instance, enhanced glacier melt increases meltwater discharge and the amplitude of diurnal discharge variations[10], increasing fluvial sediment transport capacity until peak meltwater[11] is reached. Expanded erodible area and enhanced sediment accessibility[7,12,13] with melt and thaw drive increased sediment availability. Glacier retreat facilitates sediment mobilization[14], subglacial sediment export[12,15], and mass wasting along deglaciated valley walls—increased climate-driven landslide occurrence is already evident is some cold regions[16,17]. Cryosphere degradation will likely cause a shift from a temperature-dependent sediment-transport regime[8,13,18], which has existed throughout much of the Holocene into the 20th century, to a more exclusively rainfall-dependent regime, with sediment transport dominated by rainfall-triggered mass movements[19,20].

Sediment-transport regime shifts and flux changes will have wide-reaching consequences, with some evidence of these impacts already seen. There are concerns about the impacts on water quality[21], reservoir sedimentation[10,22,23], ecological stability[24,25], and water-food-energy security for nearly 2 billion people living in or downstream of mountain areas[21,26,27]. Land-ocean biogeochemical fluxes[19,28,29,30] and contaminant transport from cryospheric basins will also change. For example, increased sediment yields from Greenland glacier outlets to the ocean impact marine ecosystems by either limiting or promoting primary productivity, due to increased turbidity and micronutrient inputs, respectively[31,32]. Accelerated thermal erosion of Arctic ice-rich permafrost coastlines, with coastal recession destroying hundreds of square kilometers of land per year[33], is impairing infrastructure and communities[34]. Importantly, abrupt permafrost thaw could mobilize large amounts of organic carbon through ground collapse, landslides and erosion[30], some of which will be delivered to fluvial and coastal systems and possibly increase aquatic CO_2 emissions and impact global carbon cycling[29,35]. The accelerating cryosphere degradation poses an urgent need for detailed assessments of sediment mobilization and transport processes in the world's cold regions.

In this Review, we present a global view of glacier mass loss and permafrost degradation and associated landscape changes. We detail the mechanisms of erosion and sediment transport in cryosphere-dominated regions and examine their responses to climate change and glacier-permafrost-snow melting at the basin scale. The observed changes in erosion and sediment yield in the world's cold regions are then synthesized. Finally, we conceptualize the likely future trends of sediment yields and discuss the related challenges, uncertainties, and opportunities.

[H1] Ongoing cryosphere degradation

The cryosphere occupies approximately 30% of the Earth's land area, and melting of snow and ice dominates sediment transport in cold regions[11]. Since the 1950s, climate-change-driven degradation of the cryosphere (for example, glacier thinning and retreat, permafrost thaw, and snowpack reduction) have changed the magnitude and frequency of glacial floods and thermokarst dynamics, impacting sediment transport regimes[36-38]. The magnitude of cryosphere change varies spatially, driven by differences in glacier and permafrost characteristics, elevation- and latitude-dependent warming rates, precipitation regime shifts, and interactions with atmospheric circulation[39,40]. This section describes these changes, grouped by glacial and permafrost processes.

[H2] Glacier mass loss and outburst floods

Although characterized by marked interannual variability and regional heterogeneity, a consistent trend of glacier recession is evident globally over the past few decades[39,41,42] (Figure 1). Worldwide, glacier mass has decreased at an estimated rate of 172±142 Gt yr^{-1} since the 1960s[41]. Annual mass loss and recession rates have accelerated in the early 21st century[41,42], with a mean annual mass loss rate of 267±16 Gt yr^{-1} or 0.39±0.12 m w.e. yr^{-1} (meters of water equivalent per year) over 2000-2019[42]. By the end of the 21st century, global glacier mass is projected to be reduced by 18–25% for the Representative Concentration Pathway (RCP) 2.6 emission scenario, with the loss of 27–33% for RCP 4.5 and 36–48% for RCP 8.5[43-45].

Since 2000, glacier mass loss has been greatest in Iceland, Alaska, the European Alps and the Southern Andes, at a rate of up to 0.88 m w.e. yr^{-1}; equivalent rates in Greenland (0.50±0.04 m w.e. yr^{-1}) are close to the global average. The smallest rates of mass loss have been observed in the Russian Arctic (0.20–0.24 m w.e. yr^{-1}) and HMA (0.21–0.24 m w.e. yr^{-1})[41,42,46]. Locally, glacier mass gains and advancing termini have been observed in Alaska[47] and the Karakoram[39] (Figure 1), likely attributable to cooler summers, increased snowfall, and the protection afforded by thick debris cover.

Rapid glacier retreat has increased the number and extent of supraglacial lakes and proglacial lakes, either ice-marginal or moraine-dammed[48] (Figure 1). The expanding glacial lakes will increase the risk of glacial lake outburst floods (GLOFs), which can cause sudden hydrogeomorphic changes and have disastrous downstream consequences[49,50] (Figure 1). From 1990 to 2018, globally the number of glacial lakes increased from 9,410 to 14,300, with their areal extent increasing from 5.93×10^3 to 8.95×10^3 km^2 ref.[48]. Larger glacial lakes are mainly located at mid-to-high latitudes, including northwestern North America, Greenland, Iceland, Scandinavia, and the Southern Andes[48]. Proglacial lakes in HMA are relatively small and clustered in northern Tien Shan and the central-to-eastern Himalaya, due to regionally faster glacier retreat there[48,51]. GLOFs occur more frequently in regions with a higher density of glacial lakes and rapid glacier recession: northwestern North America, the European Alps, the Himalaya and the Southern Andes[49,50].

[H2] Permafrost thaw and thermokarst

Atmospheric warming and earlier seasonal snowmelt thaw permafrost and increase active layer thickness (ALT)[52-54] (Figure 2). Globally, permafrost temperatures from borehole records have warmed by 0.29±0.12℃ between 2007 and 2016[52] accompanied by increasing ALT and decreasing permafrost extent. By the end of this century, even if global temperature warming was limited to 1.5℃ above pre-industrial levels, 4.8±2.2 million km^2 of permafrost (~30% of the total) would likely disappear[55]. Over half of the existing permafrost would be degraded and the active layer volume would expand by 4,910 km^3 by 2100 under the RCP 8.5[56]. Large areas of near-surface permafrost would remain only in high-latitude North America and the Russian Arctic[55,56].

Thawing of ice-rich permafrost has increased the extent of thermokarst landscapes and hillslope mass wasting[57-60], posing risks to nearby infrastructure and communities[61].From the 1990s, 20% of the circumpolar permafrost area has been disturbed by thermokarst landscapes[62] in response to the amplified regional permafrost warming rate (0.39±0.15 °C per decade)[52]. Increased incidence of thermokarst lakes, thermal erosion gullies, and retrogressive thaw slumps (RTSs) have been observed in Alaska and Siberia, where yedoma permafrost is widespread[58,63,64]. In the Canadian Arctic, RTSs now represent the dominant geomorphic change occurring over 10% of the area of northwestern Canada[65] and slump-impacted area increased fourfold around the western Canadian coasts between the 1960s and the 2000s[59]. Despite relatively slow permafrost warming (~0.2 °C per decade)[52,66], a notable expansion of slump-impacted areas has been observed in the Beiluhe region and the Qilian Mountains on the Tibetan Plateau over the past few decades[60,67].

Beyond atmospheric warming, coastal permafrost is also highly susceptible to changes in ocean temperatures and sea ice extents[68]. Along with pronounced warming of Arctic summer sea surface temperatures (~0.5°C per decade) since the 1970s[69], the sea-ice extent has declined by roughly 13% per decade[69] and the duration of the open-water period has extended by 1.5-2 times[70]. Decline in sea-ice extent is projected to continue through to the end of this century, with the annual ice-free period extending to eight months under RCP 8.5[69]. The coasts of the warming Arctic Ocean are being destroyed as warmer seawater thaws coastal ground-ice bluffs[71,72].

[H1] Changing dynamics of sediment transport

Cryosphere degradation influences sediment mobilization, transport, deposition, and delivery by modifying the magnitude and timing of hydrological and geomorphic processes, changing the nature and distribution of sediment sources and sinks, and reshaping connectivity within and between hillslopes and fluvial systems. This section discusses the response of erosion processes, sediment sources and sinks, and basin-scale sediment delivery to climate change in glacierized and permafrost regions.

[H2] Glacierized basins

As powerful erosive agents, glaciers mobilize and transport large amounts of sediment, especially in temperate mountain regions, by glacier movement, subglacial and supraglacial and ice-marginal drainage systems, and proglacial streams[73-75] (Figure 3). In partially glacierized basins, erosion and sediment transport are influenced by ice dynamics and the thermal status of the glacier, subglacial topography, bedrock lithology, glacio-hydrology, and access to stored sub- and proglacial sediment[9,31,76].

[H3] Glacial and paraglacial erosion

Quarrying and abrasion are the primary processes associated with glacial erosion and both are sensitive to temperature, glacier mass balance, and subglacial hydrology[15,77,78]. During quarrying (Number 1 on Figure 3), blocks of rock of varying sizes are plucked from the rock outcrops at the base of a glacier, forming chatter marks. If they become incorporated into the ice, they are transported down gradient by glacier sliding[79,80], creating an angular blocky coarse sediment[79]. If not transported, eroded material will accumulate on the glacier bed, forming subglacial till. Quarrying rates scale with the number of pre-existing bedrock cracks, the crack growth rate, water pressure at the glacier-bedrock interface, bedrock strength and heterogeneity, and the basal sliding velocity[78-81]. With abrasion (Number 2 on Figure 3), plucked debris embedded in the glacier sole or side erodes the underlying or adjacent bedrock as the glacier moves[82], forming striations on bedrock surfaces and producing fine-grained abraded sediment[82]. Abrasion rate is proportional to the basal sliding velocity of the glacier, the amount of basal debris, the debris-bed contact force, and the bedrock's resistance to erosion[82,83]. Abrasion and quarrying can amplify each other: abrasion is enhanced by debris generated from quarrying, and quarrying is enhanced by the abrasion-induced increase of differential stresses[74].

The overall bedrock erosion rate scales empirically with the glacier sliding velocity via a linear or power-law relationship, known as the glacial erosion law[9,31,84], although there is debate as to how non-linear this process is[77]. Glacier sliding velocity is regulated by glacier thermal regime (as a function of ice temperature and pressure), the subglacial hydrology, and glacier mass balance[74,85,86], and displays latitudinal variations[15]. Compared with cold-based polar glaciers, warm-based (also referred to as wet-based) temperate glaciers have lower ice viscosity and higher basal sliding velocities[15,87]. Glacial erosion rates range from 0.001 mm yr^{-1} for cold-based glaciers to over 100 mm yr^{-1} for fast-moving temperate glaciers[15,74,76,88]. Long-term glacier mass loss can reduce the gravitational driving force and decelerate sliding[86]. However, the warming-driven increased glacier meltwater can reach the ice-bedrock interface and temporarily increase subglacial water pressure and lubricate the glacier base, facilitating basal sliding and subglacial erosion[78,89]. While these mechanisms have been well studied[90], substantial uncertainties remain regarding controls on the processes and rates of glacial erosion[74], particularly in the capacity of temperate glaciers to evacuate eroded sediment.

In a warming atmosphere, retreating glacial snouts and ice-surface lowering can expose ice-marginal bedrock, till, and morainal debris to subaerial conditions. Adjacent debuttressed slopes can amplify paraglacial erosion by triggering landslides and rockfalls (Number 3 on Figure 3). In response to deglaciation, the magnitude and frequency of rockfalls have increased in North America, New Zealand, Norway, and the European Alps[40,91-95]. Rockfalls from exposed oversteepened slopes or lateral moraines can be triggered by active freeze-thaw weathering[96], ice segregation[97,98], alpine permafrost thaw, and intense rainfall[91,94], resulting in increases of debris and sediment accumulation on the glacier surface (Number 4 on Figure 3) and at the glacier margins[99,100].

[H3] Subglacial sediment transport

The importance of subglacial drainage systems in glacier basal sliding, subglacial erosion, and sediment transport has been increasingly emphasized[74,75,101]. Subglacial channelized drainage systems are effective in evacuating subglacially eroded sediment, especially coarse sediment[101-103], although they are spatially limited and will shrink as glaciers thin.

With increased melting, newly generated and expanded crevasses and moulins (Numbers 5–6 on Figure 3) on the surface of glaciers and ice sheets can boost surface-to-bed water transfer by forming near-vertical conduits connected to distributed englacial water routing networks[104-106]. The drainage from supraglacial lakes and streams (Number 7 on Figure 3) through preexisting englacial fractures opens new vertical hydro-connections, possibly causing transient ice-bed separation, ice uplift and water pulses, and carving new bedrock channels[107,108]. Subglacial drainage systems promoted by surface-to-bed water transfer can increase subglacial abrasion by sediment-bearing flows and effectively remove protective sediment from bedrock surfaces, although erosion rates associated with subglacial meltwater can be up to two orders of magnitude lower than those for glacial erosion[75,101]. Furthermore, subglacial lake outbursts can surcharge subglacial drainage systems, flush out subglacial sediments, and impact proglacial hydrogeomorphic environments, forming outwash fans at glacier margins and aggrading existing proglacial channels[109,110].

Access to stored amounts of sediment and till is also important in subglacial sediment evacuation[12]. Glacier equilibrium line altitudes can progressively retreat upslope during deglaciation, and the accessibility of subglacially stored sediment increases by exposing large amounts of previously buried sediment (glacial tills, Number 9 on Figure 3) to the upward extended subglacial drainage networks[12]. As the glacier equilibrium line moves upward, increased meltwater can access subglacial tills at higher elevations and remove stored sediment, promoting glacial bedrock erosion until the glacier is smaller than a critical size[12].

[H3] Sediment delivery in response to deglaciation

As glaciers retreat, they commonly leave behind abundant readily transportable sediment for a transient period (for example, decades or centuries), and then these deposits are progressively mined leaving a supply-limited environment[111]. Most of this sediment is not rapidly transferred downstream but remains as moraines, debris cones, and alluvial fans in the proglacial zone[14]. During intense melting or extreme rainstorms, this sediment deposited near the glacier terminus may be remobilized and delivered downstream[111-113].

The transport efficacy and storage of sediment mobilized by glacier erosion are largely influenced by glacier melt volume[114] and glacier-channel connectivity[7,36]. As glaciers recede, gullies extend upslope and enhance sediment connectivity and delivery by reducing dependence on supra/sub-glacial transport and expanding the contributing area[7,14,115]. However, export of glacial sediment downstream is modulated by sediment sinks (notably, proglacial lakes, Number 8 on Figure 3)[116,117] and disconnections (for example, moraines or alluvial fans)[14], creating transient disconnectivity[7,36]. Proglacial lakes have been increasing worldwide[48] and can trap large proportions of the sediment mobilized by glaciers (40–80%) and act as first-order sediment sinks[116].

Whereas proglacial lakes generally trap sediment, GLOFs are distinctive agents of sediment delivery far outpacing other erosion processes, due to the high stream power. GLOFs enhance channel erosion by mobilizing channel-defining coarse sediment and deliver large amounts of sediment downstream[118-120]. Sudden drainage of glacial lakes is often associated with order of magnitude increases in discharge[22,49,50]. Powerful streamflow pulses in a GLOF water bore mobilize and transport channel-defining boulders that are rarely affected by more conventional floods[118,119]. Once armoring boulders are removed, large amounts of unconsolidated sediment can be mobilized from the underlying river channels, accompanied by bedrock erosion and lateral riverbank erosion[121,122]. A 2016 GLOF in Nepal[118] affected a 40-km stretch of river channel by downcutting the riverbed by 1–10 m, widening the channel by 40%, causing 26 channel-connected landslides and a 30-fold increase in sediment flux. Although the substantially increased sediment flux associated with GLOFs gradually revert to near the original level, erosion and deposition during GLOFs and associated geomorphic adjustments can cause severe, long-lasting consequences downstream[119,123].

With ongoing deglaciation and commonly increased precipitation extremes[40,124], sediment yield from glacierized basins will initially increase, driven by increased glacial erosion and sediment supply[125,126], easier access to subglacial tills[12], increased transport capacity, and increased incidence of extreme floods. A subsequent sediment decrease reflects declining glacier mass and meltwater, decelerated glacial erosion[86,117], decreased freeze-thaw weathering at lower elevations[127] and vegetation colonization (Figure 3).

[H2] Permafrost basins

In response to atmospheric warming and precipitation extremes[3,65], permafrost thaw and the intensity of thermokarst erosion have intensified in many permafrost regions. The associated release and mobilization of stored sediment increase fluvial sediment loads[37,128]. Permafrost degradation impacts fluvial sediment fluxes by expanding the extent of erodible thermokarst landscapes and changing the density and spatial distribution of flow paths and therefore sediment connectivity[1,57,65,129] (Figure 4). The impact of permafrost on hydrogeomorphic processes can be subdivided into physical disturbance (Numbers 1–7 on Figure 4 showing visible landscape changes) and thermal disturbance (Number 8 on Figure 4 showing no visible geomorphic changes) [20,37,130]. Among the processes involved, active-layer detachment, thermal erosion gullies, retrogressive thaw slumps, and fluvio-thermal erosion are the primary sediment sources[13,131-133].

[H3] Permafrost erosion

Active-layer detachment (ALD) represents the occurrence of landslides on low-angled permafrost slopes with the thawed active layer sliding downslope (Number 1 on Figure 4)[134]. ALD can be initiated by deep active-layer thaw during warm summers or excessive porewater pressure caused by heavy rainfall or snowmelt[17,134,135]. Once initiated, ALDs can continue downslope for hundreds of meters, with a long-distance impact on sediment mobilization and transport[136]. Expanded scar zones with ALDs extending downslope expose the underlying permafrost and accelerate thawing[17]. The exposed ground ice can trigger thaw slumps, amplifying disturbances[137] or cause land subsidence, trapping sediment in the scar zone[136]. Newly available sediment can cause long-lasting increases in downstream sediment fluxes when transported by rainfall runoff or meltwater and sustained by hydrogeomorphic connectivity[131].

Thermal erosion gullies (TEGs) initiate by surface heat melt of ground ice and by surface flow incising into high-ice-content permafrost. TEGs commonly occur on permafrost slopes (Number 2 on Figure 4) or within eroded ice-wedge polygons (Number 6 on Figure 4) [132,138]. Once initiated, TEGs can lengthen by hundreds of meters and widen substantially through lateral erosion and headward erosion[138], because of ground ice melting[63,132,138]. Lateral and headward erosion of TEGs can trigger channel-connected permafrost collapses and slumps[137] and link upslope sediment sources with downstream river channels[138], notably increasing slope channelization and sediment supply. The shortened flow path by TEGs accelerates the response of sediment fluxes to hydrological changes and permafrost disturbance[132,135]. Additionally, vegetation and wetlands can degrade by TEG development, which can further increase erosion rates along TEGs through positive feedback[139].

Retrogressive thaw slumps (RTSs, Number 3 on Figure 4) are important sediment sources in ice-rich permafrost and are sensitive to climate change[59,129]. Increasing incidence of RTSs has been reported in permafrost environments worldwide, including the Arctic and the Tibetan Plateau, driven by atmospheric warming and increased summer rainfall[3,59,67]. RTSs show seasonal cycles and initiate in summer by melting of exposed ground ice in a headwall[3]. The meltwater then mobilizes debris and soil from the headwall[128,129]. RTSs stabilize in autumn, due to lower temperatures ceasing ice melting and accumulated sediment covering the ice[3]. RTSs can remain active and expand for years to decades, if the mobilized material continues to be transported downslope and exposed headwalls are still ice-rich[3,140]. Channel-connected RTSs have been found to increase downstream sediment loads by orders of magnitude[128,129]. Development of RTSs intensifies by extreme rainstorms[3], lateral heat exchange along riverbanks or lakeshores[141], other landscape disturbances[137], and permafrost shoreline retreat[142].

Fluvio-thermal erosion (FTE, Number 4 on Figure 4), or thermal bank erosion, is erosion by moving water that thaws frozen substrate and melts ground ice along a riverbank[143]. With earlier ice breakup, warming river water temperatures, and increasing water discharge, FTE has been increasingly observed in Alaska, Arctic Canada, and Siberia[63,144-146]. Riverbank permafrost thawing is dominated by conductive heat exchange between warmer river water and frozen banks[54,63,141]. Once FTE begins, formation of thermo-erosional niches at the base of the riverbank reduces bank stability, causing collapse[146-148]. During high flows, this readily available sediment and abundant organic matter of the typically peaty floodplain or bar surfaces can be rapidly transported by the flowing water[143] and increase sediment and carbon loads substantialy[144,145]. The efficacy and magnitude of FTE are influenced by factors including the presence of river ice, river water temperature, and discharge[145,148]. During the early melt-season, drifting ice can remove the riverbank protective layer by abrasion, undercutting, and gouging, exposing the underlying bank to fluvial entrainment[149]. For rivers of warm water, ice breakup pulses can cause FTE due to substantial increases in water levels and discharges and expanded contact with the floodwater[150,151]. FTE can also gradually stabilize due to decreased ground ice exposure caused by sediment deposition at the base of the riverbanks and on their flattened profiles[63,147].

[H3] Sediment delivery in response to thermokarst processes

Permafrost thaw expands thermokarst landscapes and creates active sediment sources[13,34,152]. The efficacy of sediment mobilization and delivery downstream from the disturbed permafrost area is governed by basin-scale hydrogeomorphic connectivity[129,153]. New gullies and expanded flow paths during intense rainfall or high meltwater increase sediment conveyance by enhancing hillslope-channel coupling, reworking previously stored sediment and linking disconnected sediment sources (for example, hillslope RTS and ALD, Figure 4)[8,129]. Such increased connectivity facilitates a sediment cascade and transmits the signal of disturbance downstream[8,19,140]. However, the signal generated by upstream permafrost disturbance and degradation can be disconnected from downstream areas and the catchment outlet by local sediment sinks, including expanded areas of thaw subsidence[136] (Number 7 on Figure 4), thermokarst lakes[58] (Number 5 on Figure 4), and debris tongues accumulating within the disturbed area[140].

Permafrost thaw can also dampen sediment transport by altering soil permeability, surface/subsurface flow paths, and hydrological connectivity[130]. Despite the likely increase of overall sediment transport capacity due to extension of the melt season, more extreme rain, and melting of ground ice, potential loss of peak meltwater capacity in the melt season due to enhanced water infiltration can decrease sediment transport capacity[154,155]. With permafrost thaw, talik enlargement and breakthrough can increase the connection between surface water and groundwater[154,156].

Permafrost disturbance will likely increase nonlinearly in a changing climate, causing disproportionate increases in fluvial fluxes and downstream impacts[3,65,140,157] until thermokarst landscapes stabilize. The continued melting of ground ice should increase sediment availability through the development of more erodible and accessible thermokarst landscapes and boost slope-channel connectivity[3,157] (Figure 4). Increased precipitation intensity[124] could intensify permafrost erosion by triggering mass movements, remobilizing deposited sediment and further accelerating permafrost thaw via lateral heat exchange[19].

[H3] Erosion along permafrost coasts

Sediment mobilization along permafrost coastlines is characterized by the complicated interplay of permafrost status and thermokarst development, sea ice extent, open-water periods, wave and storm activities, and sea level rise[68,158], making it distinct from permafrost hillslope processes. Thermo-denudation of the bluff top and thermo-abrasion of the bluff base represent the primary sediment mobilization processes from ice-rich permafrost coasts[159]. Thermo-denudation driven by intensified solar radiation and heat conduction ablates the ground ice, reduces the cohesion of ice-bonded bluff slopes, and triggers coastal recession by ALDs, RTSs, and ground subsidence[142,160]. Ice-rich bluffs can contain up to 65% ice, so most melt results in water; the remaining thawed sediment are delivered to the bluff base by meltwater and gravity[159].

In contrast, thermo-abrasion includes both thermal erosion by seawater and mechanical erosion by wave action[161] and is pronounced in coasts with high ground-ice content experiencing decreased sea ice, higher windwave energy and storm surge setup[162]. The landward recession of bluff toes during thermo-abrasion commonly forms thermo-niches and related block failures[72,163], substantially increasing coastal erosion rates and introducing sediment and carbon into the offshore system[72,159]. Erosion along ice-rich permafrost coastlines outpaces mechanical erosion along non-permafrost coasts[33,68]. The mass-wasting processes initiated by thermo-abrasion tend to dominate the erosion and shape coastal morphology along high-latitude coasts in response to ocean warming[72]. Whereas coastal bluffs can contain peaty and organic-rich layers, inventories of bluff substrate characteristics and coastal erosion rates have shown that carbon fluxes to the ocean from coastal erosion are less impactful than riverine transport[164].

[H1] Observed increases in sediment fluxes

Increased erosion and basin-scale sediment yields are observed in the world's cold regions, driven by rapid cryosphere degradation[1,4,140]. A compilation of 76 locations shows upward trends in sediment fluxes (suspended load, bedload, particulate organic carbon, and riverbank/slope erosion) from over 50 studies (Figure 5a and Supplementary Table 1). The global distribution of such evidence is influenced by established sediment-monitoring programs and published data and is biased towards suspended sediment (53 locations) with far fewer studies of bedload (15 locations) or erosion rates (8 locations; Supplementary Table 3). Observed locations do provide evidence from the high Arctic, European mountains, HMA and Andes (Figure 5a). Few studies documented decreased sediment fluxes (for example, the Swiss Alps and northern Alaska)[147,165] (Supplementary Figure 2), which could reflect field sampling bias toward regions where negative impacts of increasing sediment flux were suspected.

[H2] Observations from thermokarst basins

Expanding thermokarst landscapes are thought to be responsible for increased riverbank erosion and sediment yields from the Canadian and Siberian Arctic, Alaska, and the Tibetan Plateau (Figure 5a), the released organic carbon and nutrients further impacting thermokarst ecosystems[30,166]. In the eastern Lena Delta, erosion rates along yedoma permafrost riverbanks increased three-fold between the 1960s and 2010s and the amount of organic carbon and nitrogen released into the rivers more than doubled[167]. Along an actively eroded bluff (150-m) of the Itkillik River in Alaska, the yedoma riverbank retreated at an accelerated rate, reaching 20 m yr^{-1} between 2007 and 2011, and annually released ~70,000 t of sediment (including 880 t of organic carbon) into the river[63]. Channel-connected thaw slumps in northern Canada have increased sediment yields by up to three orders of magnitude compared to undisturbed basins[128,129,140]. Active-layer detachments reported from small watersheds in the Canadian High Arctic (Melville Island) caused a 30-fold increase in sediment flux during an anomalously warm year, followed by multiyear recovery[131]. In the Tibetan Plateau, permafrost thawing and associated expansion of erodible landscapes have doubled the sediment yield in a headwater of the Yangtze between 1985 and 2016[168]; and led to an 8-fold increase in sediment yield around Qinghai Lake between the 1990s and 2010s[169].

[H2] Observations from glacierized basins

Increased erosion and sediment yields from European mountains, the Himalaya, and the Andes are mainly induced by increased subglacial sediment evacuation and unstable hillslopes (Figure 5a), threatening downstream infrastructure and communities[23,170,171]. In the Italian Alps, warming temperatures have been locally linked to an order-of-magnitude increase in erosion from high periglacial terrain[172]. A near doubling of coarse sediment yield has been observed in two partially glacierized basins in the western Swiss Alps in response to glacier recession[7,36]. In Norway, the sedimentation rate of a proglacial lake has accelerated since the 1970s in response to accelerating glacier retreat[173]. In European mountains, increased reservoir sedimentation has reduced the lifetime of hydropower infrastructure and more frequent sediment flushing of hydropower installations has demonstrated negative impacts on instream ecosystems[171]. In the Chandra River, western Himalaya, the sediment yield doubled between the 1980s and 2010s, associated with a 65% reduction in low-elevation glacier volumes[174]. The increased channel and floodplain deposition in less-steep areas downstream can elevate the riverbed and potentially trigger river avulsions and flooding[170,175]. Rapid glacier recession in the Southern Andes has caused a 6-fold increase in frequency of extreme turbidity events, affecting water quality in the nearby megacity of Santiago[23]. Although sediment yields in response to longer-term deglaciation since the Last Glacial Maximum have rarely been observed globally, state-of-the-art conceptual models[75,176,177] and sediment-core analysis[178,179] show nonlinear increases in erosion and sediment-related yield in the early phase of deglaciation, followed by rapid decline late in deglaciation as landscapes stabilize.

[H2] Observations from polar basins

Extensive erosion has occurred along Arctic coastlines due to rapid thawing of ice-rich permafrost[33,68,158,161], with sediment-associated nutrient inputs sustaining 20% of the net primary production of the Arctic Ocean[180]. Since the early 21st century, amplified atmospheric warming has accelerated erosion rates in 18 out of 20 coastal permafrost locations in Alaska, northwestern Canada, and the East Siberian Arctic (Figure 5a,c and Table S2), enhancing land–ocean biogeochemical fluxes[180] but threatening coastal infrastructure[158,161,181]. Specifically, a seven-fold increase in coastal erosion rate has been observed along the Barents Sea coast (Western Russian Arctic) between the 1960s and 2000s[182]. Erosion rates along the Beaufort Sea coast (Alaskan Arctic) and Herschel Island (Canadian Arctic) have doubled since the 1950s[163,183] and accelerated erosion is amplified by the increased incidence of coast-connected thermokarst landslides (~140%)[142]. Erosion and irreversible land loss costing billions of dollars for relocating or protecting infrastructure[34,161], and conflict with future anticipated economic development of the Arctic coastline, including the expansion of ports and shipping, and oil and gas exploitation.

Mass loss from the Greenland Ice Sheet since the 1960s has caused a 56% increase in suspended-sediment delivery to adjacent proglacial rivers and coastal zones[31,184]. The increased sediment flux outpaces delta erosion and stagnation due to sea level rise[4,185,186], thus prograding the deltas of southern Greenland by 110% between the 1940s and 2010s[4] (Figure 5d). The progradation of Greenland's deltas emphasizes the role of land–ocean sediment flux in sustaining deltas and what could be seen as a longer-term benefit of terrestrial cryosphere degradation[4,187].

[H1] Projections and peak sediment

Ongoing climate change will likely initially increase sediment yields in pristine cold environments, in response to glacier melting and permafrost thaw. Sediment yield will eventually reach a maximum[75,117,176], herein referred to as "peak sediment", followed by declining sediment yields as the areas contributing sediment shrink. Ongoing cryosphere degradation will also cause a shift in the sediment transport regime and seasonal pattern[37,188]. The timing of the sediment regime shift and the tipping point of sediment yield will be jointly regulated by trends in meltwater runoff, erosive rainfall and the extent of thermally-controlled erodible landscapes and ice-free erodible landscapes[6,75,88,111] (Fig. 7). This section qualitatively speculates on the likely evolution of future sediment yield in response to global warming in large cryospheric basins.

Globally, nearly half of the large-scale glacierized basins have already passed peak meltwater and entered the declining meltwater phase; the tipping points in most remaining basins are projected to be reached before 2100[11]. The completion of deglaciation could occur after the year 2200, with Arctic and Antarctic ice sheets and Arctic permafrost existing beyond 2200[189-191]. Compared with the hydrological impacts of deglaciation, landscape changes are understudied and more complex to project[88]. Theoretically, active thermally-controlled erodible landscapes, as a function of temperature and ice content (glacier or ground ice)[13], will peak at the time of peak meltwater and then decline to zero at the completion of deglaciation, concurrently with ice-free erodible landscapes expanding. Once a zone becomes ice-free, landscapes stabilize at differing rates depending on the deglaciated landforms, geomorphic feedbacks, and landcover changes[177,192].

By reflecting changes in meltwater and erodible landscapes, sediment-transport regimes could shift through three temporal stages separated by the timing of peak meltwater and completion of deglaciation (Fig. 7), regardless of glacier re-advance, (dis-)connectivity changes, scale and/or threshold effects in sediment transport, the stabilization rate of deglaciated landscapes, and human interference. In stage I, the sediment regime is dominated by thermal processes, including thermally activated glacier/permafrost erosion and meltwater-driven sediment transport[13,18,193]. Readily erodible sediment from freshly deglaciated regions and thermokarst hillslopes, combined with enhanced transport capacity by meltwater, will likely increase sediment yield in the early stage of deglaciation[75,88]. In stage II, reduced meltwater would render rainfall-runoff increasingly important in sediment mobilization and transport and the sediment regime would be controlled by coupled thermal and pluvial processes[19]. The trend of changes in sediment yield would reflect the interplay of reduced meltwater, continuously exposed proglacial and/or periglacial sediment sources, and changes in erosive rainfall[11,177]. In stage III, fully exposed erodible ice-free landscapes and depleted meltwater after the completion of deglaciation would shift the sediment transport regime towards a precipitation-dependent regime with pluvially controlled sediment mobilization, followed by an eventual decline in sediment yield due to sediment supply exhaustion[176,177]. Evacuation of stored sediment could depend heavily on the magnitude and duration of episodic events triggered by intense rainfall and extreme floods[75,188]. Para-glaciation and mass wasting will dominate sediment supply and transport during stage III[120,176,192].

The timing of peak sediment (scenario B in Fig. 7) could occur in stage II under a stable precipitation scenario. The peak of sediment delivery may lag decades to hundreds of years behind peak meltwater, reflecting the increase in remobilization of paraglacial and subglacial sediment storage[12,125,194]; such a lag is likely to be scale dependent, being shorter (years) close to the source region and much longer (decades to centuries) farther downstream[194]. With decreasing erosive rainfall, peak sediment could arrive earlier than peak meltwater (scenario A in Fig. 7), because increased accessibility to sediment supply would not compensate for reduced erosivity and transport capacity[195]. The increasing erosive rainfall could still constrain the peak sediment within stage II, accompanied by increased sediment yield and amplified variability through the remobilization of legacy sediment inherited from paraglacial environments[19,188] (scenario C in Fig. 7).

[H1] Challenges and complexity

Long-term field observations of erosion, sediment yield, and the environmental drivers of sediment fluxes are lacking in cold regions[21,88,196,197], particularly for bedload and erosion rates. Access to the few available records is restricted by policy and technical barriers, and therefore little synthesis has been undertaken. Research biases likely exist—decreased sediment yield or reduced erosion could occur in some cryospheric basins, but few studies report such results[68]. Such limitations hamper the holistic assessment of geomorphic changes, spatio-temporal variations in sediment dynamics, and the response of basin-scale sediment yield to climate change[21,88]. The lack of field observations also impedes the development and application of sediment-yield models, due to the paucity of validation and calibration data and poor parameterization of key geomorphic processes[198,199].

Challenges and uncertainties in sediment yield modeling and future projections also arise from the inherent complexity of geomorphic processes, characterized by scale effects on sediment transport[199,200], episodic events[201], nonlinear responses of geomorphic processes[6,202], and climate feedbacks associated with cryosphere degradation[203,204]. Erosion and deposition processes vary across spatial scales and the relative importance of factors controlling sediment dynamics are scale-dependent[199,205]. For example, climate, topography, and catchment area can dominate global-scale variation of sediment yield[206], but their influences on sediment yield can be obscured by local glacier dynamics, the extent of thermokarst landscapes, and sediment connectivity[153,207,208].

Low-frequency and high-magnitude episodic sediment events (for example, mass wasting and GLOFs) can mobilize huge amounts of sediment during a short period, causing notable variability in both seasonal and annual sediment yields[201]. The frequency and duration of such extreme sediment events are difficult to predict[3,88]. Putting event data into a synthesis framework of "geomorphic work", as proposed by Wolman and Miller in 1960 may shed light on this aspect of complexity[209]. However, another complication is that cryospheric regions generally owe their high altitude and steep topography to tectonic forces, and so seismically generated landslides and sediment movement can confound detection of climatic signals—examples of earthquake-generated landslides abound in the Himalaya, Alaska, New Zealand, and the Andes[16,94,210].

Geomorphic responses to climate change can also be complicated by threshold effects, antecedent conditions, and response time-lags[21,202,211], thus precluding simulations by linear forcing-response models or universal constants[6]. Thresholds in geomorphic changes (for example, landslides) and related sediment mobilization can involve nonlinear and dynamic relationships between environmental drivers and geomorphic response[212,213]. Simulating such nonlinear and dynamic processes represent important challenges in earth surface modeling, because of their spatio-temporal heterogeneity and sensitivity to the intrinsic properties of geomorphic systems and extrinsic drivers[192,213], and the disproportionate amplification of geomorphic changes and sediment transport when thresholds are exceeded[21,211].

Furthermore, melting and thawing of the cryosphere can amplify the atmospheric warming and impact the monsoon precipitation through feedback linked to permafrost carbon[30], snow and ice albedo[204], and land-sea temperature gradients[214]. These positive feedbacks add important uncertainties to climate model projections[40,204] and likely lead to underestimation when predicting future atmosphere warming, fluvial events, and extreme sediment yields[124,215].

In a warmer future, basin-scale sediment source-to-sink processes and sediment routing systems can be altered by spatial reorganization of sediment sources and/or sinks and river channels[5,216], changing lateral and longitudinal connectivity[153], geomorphic feedbacks[7], and human activities[27,217] (Figure 6). With glacier melt and permafrost thaw, rockfalls and landslides will likely increase[100,188]. Increased slope failures could trigger GLOFs and temporarily convert glacial lakes from effective long-term sediment sinks into important sediment sources and transfer pathways, causing channel and valley erosion[118].

In efficient, well-connected pristine sediment-routing systems, intensified sediment transport leads to delta progradation[4] and increased terrestrial fluxes to the ocean (for example, Arctic deltas)[218] (Figure 6). However, in most cases, only a small fraction of the sediment mobilized from mountain headwaters impacted by cryosphere degradation will be transported downstream to basin outlets[200], and the signals of climate-change-driven increases in sediment flux from the mountain erosion zone are attenuated by the buffering effects of floodplains and sediment sinks[73,153]. The concomitant processes of fluvial sorting, coarse sediment accumulation, and formation of debris fans can cause sediment dis-connectivity[7] and buffer the downstream propagation of the sediment signal[7,14]. Increased human activity (for example, damming and sand mining) can also mute the signal of increased sediment loads from pristine uplands and even lead to delta subsidence[217].

Long-term changes in the cryosphere and sediment fluxes can lead to river reorganization, change sediment delivery pathways and dramatically alter downstream drainage networks[5,219] (Figure 6). However, the timing and intensity of river reorganization are impacted by preconditions and the episodic nature of key triggers[175]. The upslope retreat of the Kaskawulsh Glacier in the Yukon redirected one headwater stream into another river in 2016 and this river piracy had far-reaching downstream hydrogeomorphic implications[5]. Increased sediment deposition at mountain outlets in Himalayan, Andean, and southwest New Zealand foreland basins has caused river avulsions and course-shifting during floods[175,219], redistributing the water and sediment on floodplains[219]. The potential increases in river reorganization events in a warming future could further increase the uncertainty in large-scale sediment yield predictions[175,220].

The impacts of land-cover changes on sediment transport vary spatially[221-223]. Vegetation development in proglacial areas stabilizes slopes[222], but this is also complicated by deglaciation-triggered slope instability and increases in erosive rainfall[135,221]. The overall greening in a warming Northern Hemisphere[224] and vegetation restoration in particular basins[222,225] contrast with local vegetation removal due to increased slope failures[13,128,135]. The net effect of landcover changes on sediment yield remains largely unknown.

[H1] Summary and future perspectives

Amplified atmospheric warming and the resulting melting and thawing of the cryosphere have markedly altered erosion and sediment delivery from the Earth's cryospheric basins[1,4,188]. The associated increased sediment yields have caused severe consequences for aquatic ecosystems, hazards and livelihoods[21,22,175,180], but the public is still largely unprepared to deal with them. In this Review, we compiled information for the first time on changing sediment fluxes from 76 locations (covering the high Arctic, European mountains, HMA and the Andes) with increased erosion (8) and sediment yields (68) and 18 locations along Arctic coasts (Figure 5). Increased sediment yields result from the increased glacier bedrock erosion caused by increased meltwater and changes in basal sliding, the increased permafrost erosion caused by thermokarst landscape expansion, rock disintegration during deglaciation, and increases in sediment accessibility due to the exposure of underlying sediment stores and the initiation of new flow paths. However, the signal of sediment mobilization and transport can be moderated by increased sediment storage and reduced delivery efficacy due to the presence of sediment sinks, some of those (for example, hillslope-based debris fans) developing in response to increased erosion. Increases in sediment yield in most cryospheric basins are likely to continue in the next decades, with continued glacier melt and permafrost thaw, until the maximum sediment yield is reached. We pose that the timing of peak sediment is jointly regulated by changes in meltwater runoff, erosive rainfall and landscape erodibility (Fig. 7). To better assess the impacts of changing erosion and sediment yields on the functions and services of riverine and coastal ecosystems[68], biogeochemical cycles[62], terrestrial-coastal landscape evolution[6], and infrastructure systems[22], we highlight the pressing need to integrate multiple-sourced sediment observations, to develop physics-based sediment transport models that include climatic feedbacks, and to promote interdisciplinary scientific collaboration.

Current understanding and assessment of the long-term response of erosion and sediment yields to climate-driven cryosphere changes remain incomplete. Sediment monitoring is lacking in most rivers (sediment loads are measured in < 10% of the world's rivers)[217] and decadal-scale sediment observations for cryospheric basins are even rarer[2]. Apart from expanding the traditional *in-situ* sediment observations (for example, manual sediment sampling, automated sampling, and turbidity monitoring)[23,168], advances in remote sensing offer the opportunity to monitor sediment automatically and continuously and to reconstruct the temporal trends of erosion rates and sediment yields[120]. Breakthroughs in constraining relationships between surface reflectance and suspended sediment concentration and extending retrieval algorithms worldwide beyond the calibration regions will permit sediment information to be deciphered and extracted from previously unexploited satellite image archives, helping to fill the observation gaps[31,226] through making available more remote gauging stations[227]. The availability of satellite- and drone-observed images with a higher spatio-temporal resolution[228] and new techniques (for example, Structure-from-Motion photogrammetry)[227] will greatly improve the accuracy and precision of river pixels and further increase monitoring capabilities relating to sediment dynamics[3,5,144,226]. Optimization of calculating efficiency and access to the wide-ranging remotely sensed resources within the Google Earth Engine will lead to near-real-time sediment monitoring[227].

Ongoing developments in geochronology provide novel approaches to obtain information from sediment. For example, lakes can record the long-term sedimentary history across decades to thousands of years[120,227] and this history can be reconstructed by using radioactive chronometers including Caesium-137 (^{137}Cs), Radiocarbon (^{14}C), and Lead 210 (^{210}Pb) to provide a chronology[229]. New technology in sediment-core collection and analysis will reveal the response of upstream water–sediment dynamics and lake sedimentation to deglaciation[173,230]. Although cosmogenic nuclides (for example, Beryllium-10, ^{10}Be) cannot reveal temporal changes in sediment yield due to their long half-lives, they can provide estimates of millennial-scale denudation rates and help to diagnose the sediment sources[99,178]. More investigations involving cosmogenic nuclide-derived millennial-scale denudation rates could provide a benchmark, thus underpinning the evaluation of current or future changes in denudation rates[99,120]. Additionally, progress in environmental seismology can promote near real-time sediment-transport and geomorphic analysis during extreme events such as GLOFs[118,231]; advances in sediment source fingerprinting can provide information on sediment sources to unravel the relative importance of different denudational processes[112].

Physics-based sediment yield models can offer valuable insights into past and future sediment dynamics in response to climate change and cryosphere degradation and can integrate sediment delivery processes into Earth System models to provide a better representation of land-ocean nutrient and carbon cycling. Existing sediment yield models are mostly empirical or conceptual models (for example, SWAT, WBMsed[232], HydroTrend[233], BQART[206], and SAT[8]). Physics-based models are rare (for example, Water-Erosion-Prediction-Project[234]) and only marginally account for the temperature-dependent erosional processes in cryospheric basins. A fully distributed physics-based sediment-yield model that explicitly incorporates the various thermally and pluvially driven sediment mobilization and transport processes is urgently needed to simulate sediment yields from cryospheric basins at a high spatio-temporal resolution. Changes in both erosion and depositional sinks and associated changes in sediment connectivity[14,132,153] need to be considered in sediment-yield models, in order to evaluate the net effect of landscape changes in response to cryosphere degradation. By integrating deglaciation, thermokarst erosion, frost cracking, and shifts in sediment transport regimes, such models would advance the prediction of long-term sediment yields (including future systematic shifts in sediment mobilization and transport).

State-of-the-art geoscientific machine learning approaches offer an opportunity to address the challenges of data assimilation and spatio-temporal dynamics posed by the explosive growth of input data from multiple-sourced climate-cryosphere-hydrogeomorphology observations[235,236]. Additionally, coupling sediment-yield models with Earth System models would address constraints associated with representing sediment-related carbon and nutrient dynamics at large scales and better capture biogeochemical cycles and their feedbacks[237].

To advance a holistic understanding of sediment dynamics in the world's cold environments, the innovative system approach would best come from the creation of an interdisciplinary collaborative initiative, where climatologists, ecologists, glaciologists, permafrost scientists, hydrologists, civil engineers, and geomorphologists work together to establish an integrated cryosphere-water-sediment-environment observation platform that facilitates the development of fully distributed physics-based sediment-yield models. Furthermore, dialogues and collaboration between international scientists, stakeholders, local communities, and policymakers would help to bridge the gaps between state-of-the-art scientific findings and practicable adaptation strategies. Such collaboration and dialogues would help address climate change driven sediment issues and problems and facilitate the establishment of sustainable and climate-resilient infrastructure systems and riparian and coastal ecosystems in strategically important cold regions.

References:

1 Li, D. *et al.* Exceptional increases in fluvial sediment fluxes in a warmer and wetter High Mountain Asia. *Science* **374**, 599-603, doi:doi:10.1126/science.abi9649 (2021).

2 Syvitski, J. *et al.* Earth's sediment cycle during the Anthropocene. *Nature Reviews Earth & Environment*, doi:10.1038/s43017-021-00253-w (2022).

3 Lewkowicz, A. G. & Way, R. G. Extremes of summer climate trigger thousands of thermokarst landslides in a High Arctic environment. *Nat Commun* **10**, 1329, doi:10.1038/s41467-019-09314-7 (2019).

4 Bendixen, M. *et al.* Delta progradation in Greenland driven by increasing glacial mass loss. *Nature* **550**, 101-104, doi:10.1038/nature23873 (2017).

5 Shugar, D. H. *et al.* River piracy and drainage basin reorganization led by climate-driven glacier retreat. *Nature Geoscience* **10**, 370-375, doi:10.1038/ngeo2932 (2017).

6 Knight, J. & Harrison, S. The impacts of climate change on terrestrial Earth surface systems. *Nature Climate Change* **3**, 24-29, doi:10.1038/nclimate1660 (2012).

7 Lane, S. N., Bakker, M., Gabbud, C., Micheletti, N. & Saugy, J.-N. Sediment export, transient landscape response and catchment-scale connectivity following rapid climate warming and Alpine glacier recession. *Geomo* **277**, 210-227, doi:10.1016/j.geomorph.2016.02.015 (2017).

8 Zhang, T., Li, D., Kettner, A. J., Zhou, Y. & Lu, X. Constraining Dynamic Sediment-Discharge Relationships in Cold Environments: the Sediment-Availability-Transport (SAT) Model. *Water Resources Research*, doi:10.1029/2021wr030690 (2021).

9 Herman, F. *et al.* Erosion by an Alpine glacier. *Science* **350**, 193-195, doi:doi:10.1126/science.aab2386 (2015).

10 Lane, S. N. & Nienow, P. W. Decadal-Scale Climate Forcing of Alpine Glacial Hydrological Systems. *Water Resources Research* **55**, 2478-2492, doi:10.1029/2018wr024206 (2019).

11 Huss, M. & Hock, R. Global-scale hydrological response to future glacier mass loss. *Nature Climate Change* **8**, 135-140, doi:10.1038/s41558-017-0049-x (2018).

12 Delaney, I. & Adhikari, S. Increased Subglacial Sediment Discharge in a Warming Climate: Consideration of Ice Dynamics, Glacial Erosion, and Fluvial Sediment Transport. *Geophysical Research Letters* **47**, doi:10.1029/2019gl085672 (2020).

13 Li, D., Overeem, I., Kettner, A. J., Zhou, Y. & Lu, X. Air Temperature Regulates Erodible Landscape, Water, and Sediment Fluxes in the Permafrost-Dominated Catchment on the Tibetan Plateau. *Water Resources Research* **57**, e2020WR028193, doi:10.1029/2020WR028193 (2021).

14 Mancini, D. & Lane, S. N. Changes in sediment connectivity following glacial debuttressing in an Alpine valley system. *Geomo* **352**, doi:10.1016/j.geomorph.2019.106987 (2020).

15 Koppes, M. *et al.* Observed latitudinal variations in erosion as a function of glacier dynamics. *Nature* **526**, 100-103, doi:10.1038/nature15385 (2015).

16 Kirschbaum, D., Kapnick, S. B., Stanley, T. & Pascale, S. Changes in Extreme Precipitation and Landslides

Over High Mountain Asia. *Geophysical Research Letters* **47**, e2019GL085347, doi:https://doi.org/10.1029/2019GL085347 (2020).

17 Patton, A. I., Rathburn, S. L., Capps, D. M., McGrath, D. & Brown, R. A. Ongoing Landslide Deformation in Thawing Permafrost. *Geophysical Research Letters* **48**, doi:10.1029/2021gl092959 (2021).

18 Syvitski, J. P. M. Sediment discharge variability in Arctic rivers: implications for a warmer future. *Polar Res.* **21**, 323-330, doi:10.3402/polar.v21i2.6494 (2002).

19 Beel, C. R. *et al.* Emerging dominance of summer rainfall driving High Arctic terrestrial-aquatic connectivity. *Nat Commun* **12**, 1448, doi:10.1038/s41467-021-21759-3 (2021).

20 Patton, A. I., Rathburn, S. L. & Capps, D. M. Landslide response to climate change in permafrost regions. *Geomo* **340**, 116-128, doi:10.1016/j.geomorph.2019.04.029 (2019).

21 East, A. E. & Sankey, J. B. Geomorphic and Sedimentary Effects of Modern Climate Change: Current and Anticipated Future Conditions in the Western United States. *Reviews of Geophysics* **58**, doi:10.1029/2019rg000692 (2020).

22 Li, D. *et al.* High Mountain Asia hydropower systems threatened by climate-driven landscape instability. *Nature Geoscience*, doi:10.1038/s41561-022-00953-y (2022).

23 Vergara, I., Garreaud, R. & Ayala, Á. Sharp Increase of Extreme Turbidity Events Due To Deglaciation in the Subtropical Andes. *Journal of Geophysical Research: Earth Surface* **127**, doi:10.1029/2021jf006584 (2022).

24 Hopwood, M. J. *et al.* Non-linear response of summertime marine productivity to increased meltwater discharge around Greenland. *Nat Commun* **9**, 3256, doi:10.1038/s41467-018-05488-8 (2018).

25 Yi, Y., Liu, Q., Zhang, J. & Zhang, S. How do the variations of water and sediment fluxes into the estuary influence the ecosystem? *Journal of Hydrology* **600**, doi:10.1016/j.jhydrol.2021.126523 (2021).

26 Immerzeel, W. W. *et al.* Importance and vulnerability of the world's water towers. *Nature* **577**, 364-369, doi:10.1038/s41586-019-1822-y (2020).

27 Best, J. Anthropogenic stresses on the world's big rivers. *Nature Geoscience* **12**, 7-21, doi:10.1038/s41561-018-0262-x (2019).

28 Li, X. *et al.* Globally elevated chemical weathering rates beneath glaciers. *Nature Communications* **13**, doi:10.1038/s41467-022-28032-1 (2022).

29 Hilton, R. G. & West, A. J. Mountains, erosion and the carbon cycle. *Nature Reviews Earth & Environment* **1**, 284-299, doi:10.1038/s43017-020-0058-6 (2020).

30 Turetsky, M. R. *et al.* Carbon release through abrupt permafrost thaw. *Nature Geoscience* **13**, 138-143, doi:10.1038/s41561-019-0526-0 (2020).

31 Overeem, I. *et al.* Substantial export of suspended sediment to the global oceans from glacial erosion in Greenland. *Nature Geoscience* **10**, 859-863, doi:10.1038/ngeo3046 (2017).

32 Arrigo, K. R. *et al.* Melting glaciers stimulate large summer phytoplankton blooms in southwest Greenland waters. *Geophysical Research Letters* **44**, 6278-6285, doi:10.1002/2017gl073583 (2017).

33 Lantuit, H. *et al.* The Arctic Coastal Dynamics Database: A New Classification Scheme and Statistics on Arctic Permafrost Coastlines. *Estuaries and Coasts* **35**, 383-400, doi:10.1007/s12237-010-9362-6 (2012).

34 Hjort, J. *et al.* Degrading permafrost puts Arctic infrastructure at risk by mid-century. *Nat Commun* **9**, 5147, doi:10.1038/s41467-018-07557-4 (2018).

35 Wild, B. *et al.* Rivers across the Siberian Arctic unearth the patterns of carbon release from thawing permafrost. *Proc Natl Acad Sci U S A* **116**, 10280-10285, doi:10.1073/pnas.1811797116 (2019).

36 Micheletti, N. & Lane, S. N. Water yield and sediment export in small, partially glaciated Alpine watersheds in a warming climate. *Water Resources Research* **52**, 4924-4943, doi:10.1002/2016wr018774 (2016).

37 Beel, C. R. *et al.* Differential impact of thermal and physical permafrost disturbances on High Arctic

dissolved and particulate fluvial fluxes. *Sci Rep* **10**, 11836, doi:10.1038/s41598-020-68824-3 (2020).

38 Shugar, D. H. *et al.* A massive rock and ice avalanche caused the 2021 disaster at Chamoli, Indian Himalaya. *Science* **373**, 300-306, doi:doi:10.1126/science.abh4455 (2021).

39 Farinotti, D., Immerzeel, W. W., de Kok, R., Quincey, D. J. & Dehecq, A. Manifestations and mechanisms of the Karakoram glacier Anomaly. *Nat Geosci* **13**, 8-16, doi:10.1038/s41561-019-0513-5 (2020).

40 Hock, R., G. *et al.* High Mountain Areas: In: IPCC Special Report on the Ocean and Cryosphere in a Changing Climate. (2019).

41 Zemp, M. *et al.* Global glacier mass changes and their contributions to sea-level rise from 1961 to 2016. *Nature* **568**, 382-386, doi:10.1038/s41586-019-1071-0 (2019).

42 Hugonnet, R. *et al.* Accelerated global glacier mass loss in the early twenty-first century. *Nature* **592**, 726-731, doi:10.1038/s41586-021-03436-z (2021).

43 Hock, R. *et al.* GlacierMIP – A model intercomparison of global-scale glacier mass-balance models and projections. *JGlac* **65**, 453-467, doi:10.1017/jog.2019.22 (2019).

44 Marzeion, B. *et al.* Partitioning the Uncertainty of Ensemble Projections of Global Glacier Mass Change. *Earth's Future* **8**, doi:10.1029/2019ef001470 (2020).

45 Huss, M. & Hock, R. A new model for global glacier change and sea-level rise. *Frontiers in Earth Science* **3**, doi:10.3389/feart.2015.00054 (2015).

46 Ciracì, E., Velicogna, I. & Swenson, S. Continuity of the Mass Loss of the World's Glaciers and Ice Caps From the GRACE and GRACE Follow-On Missions. *Geophysical Research Letters* **47**, doi:10.1029/2019gl086926 (2020).

47 Truffer, M., Motyka, R. J., Hekkers, M., Howat, I. M. & King, M. A. Terminus dynamics at an advancing glacier: Taku Glacier, Alaska. *JGlac* **55**, 1052-1060, doi:10.3189/002214309790794887 (2009).

48 Shugar, D. H. *et al.* Rapid worldwide growth of glacial lakes since 1990. *Nature Climate Change* **10**, 939-945, doi:10.1038/s41558-020-0855-4 (2020).

49 Carrivick, J. L. & Tweed, F. S. A global assessment of the societal impacts of glacier outburst floods. *Global and Planetary Change* **144**, 1-16, doi:10.1016/j.gloplacha.2016.07.001 (2016).

50 Veh, G. *et al.* Trends, Breaks, and Biases in the Frequency of Reported Glacier Lake Outburst Floods. *Earth's Future* **10**, doi:10.1029/2021ef002426 (2022).

51 Li, X. *et al.* Climate change threatens terrestrial water storage over the Tibetan Plateau. *Nature Climate Change*, doi:10.1038/s41558-022-01443-0 (2022).

52 Biskaborn, B. K. *et al.* Permafrost is warming at a global scale. *Nat Commun* **10**, 264, doi:10.1038/s41467-018-08240-4 (2019).

53 Gruber, S. *et al.* Review article: Inferring permafrost and permafrost thaw in the mountains of the Hindu Kush Himalaya region. *The Cryosphere* **11**, 81-99, doi:10.5194/tc-11-81-2017 (2017).

54 Smith, S. L., O'Neill, H. B., Isaksen, K., Noetzli, J. & Romanovsky, V. E. The changing thermal state of permafrost. *Nature Reviews Earth & Environment* **3**, 10-23, doi:10.1038/s43017-021-00240-1 (2022).

55 Chadburn, S. E. *et al.* An observation-based constraint on permafrost loss as a function of global warming. *Nature Climate Change* **7**, 340-344, doi:10.1038/nclimate3262 (2017).

56 Overeem, I. *et al.* A modeling toolbox for permafrost landscapes. *Eos, Transactions American Geophysical Union (Online)* **99** (2018).

57 Farquharson, L. M. *et al.* Climate Change Drives Widespread and Rapid Thermokarst Development in Very Cold Permafrost in the Canadian High Arctic. *Geophysical Research Letters* **46**, 6681-6689, doi:10.1029/2019gl082187 (2019).

58 Veremeeva, A., Nitze, I., Günther, F., Grosse, G. & Rivkina, E. Geomorphological and Climatic Drivers of

Thermokarst Lake Area Increase Trend (1999–2018) in the Kolyma Lowland Yedoma Region, North-Eastern Siberia. *Remote Sensing* **13**, doi:10.3390/rs13020178 (2021).
59 Segal, R. A., Lantz, T. C. & Kokelj, S. V. Acceleration of thaw slump activity in glaciated landscapes of the Western Canadian Arctic. *Environmental Research Letters* **11**, doi:10.1088/1748-9326/11/3/034025 (2016).
60 Mu, C. *et al.* Acceleration of thaw slump during 1997–2017 in the Qilian Mountains of the northern Qinghai-Tibetan plateau. *Landslides* **17**, 1051-1062, doi:10.1007/s10346-020-01344-3 (2020).
61 Hjort, J. *et al.* Impacts of permafrost degradation on infrastructure. *Nature Reviews Earth & Environment* **3**, 24-38, doi:10.1038/s43017-021-00247-8 (2022).
62 Olefeldt, D. *et al.* Circumpolar distribution and carbon storage of thermokarst landscapes. *Nat Commun* **7**, 13043, doi:10.1038/ncomms13043 (2016).
63 Kanevskiy, M. *et al.* Patterns and rates of riverbank erosion involving ice-rich permafrost (yedoma) in northern Alaska. *Geomo* **253**, 370-384, doi:10.1016/j.geomorph.2015.10.023 (2016).
64 Jones, B. M. *et al.* Lake and drained lake basin systems in lowland permafrost regions. *Nature Reviews Earth & Environment* **3**, 85-98, doi:10.1038/s43017-021-00238-9 (2022).
65 Kokelj, S. V., Lantz, T. C., Tunnicliffe, J., Segal, R. & Lacelle, D. Climate-driven thaw of permafrost preserved glacial landscapes, northwestern Canada. *Geology* **45**, 371-374, doi:10.1130/g38626.1 (2017).
66 Cheng, G. *et al.* Characteristic, changes and impacts of permafrost on Qinghai-Tibet Plateau. *Chinese Science Bulletin* **64**, 2783-2795 (2019).
67 Luo, J., Niu, F., Lin, Z., Liu, M. & Yin, G. Recent acceleration of thaw slumping in permafrost terrain of Qinghai-Tibet Plateau: An example from the Beiluhe Region. *Geomo* **341**, 79-85, doi:10.1016/j.geomorph.2019.05.020 (2019).
68 Irrgang, A. M. *et al.* Drivers, dynamics and impacts of changing Arctic coasts. *Nature Reviews Earth & Environment* **3**, 39-54, doi:10.1038/s43017-021-00232-1 (2022).
69 Pörtner, H.-O. *et al.* The ocean and cryosphere in a changing climate. *IPCC Special Report on the Ocean and Cryosphere in a Changing Climate* (2019).
70 Barnhart, K. R., Miller, C. R., Overeem, I. & Kay, J. E. Mapping the future expansion of Arctic open water. *Nature Climate Change* **6**, 280-285, doi:10.1038/nclimate2848 (2015).
71 Maslakov, A. & Kraev, G. Erodibility of permafrost exposures in the coasts of Eastern Chukotka. *Polar Science* **10**, 374-381, doi:10.1016/j.polar.2016.04.009 (2016).
72 Jones, B. M. *et al.* A decade of remotely sensed observations highlight complex processes linked to coastal permafrost bluff erosion in the Arctic. *Environmental Research Letters* **13**, doi:10.1088/1748-9326/aae471 (2018).
73 Jaeger, J. M. & Koppes, M. N. The role of the cryosphere in source-to-sink systems. *Earth-Sci. Rev.* **153**, 43-76, doi:10.1016/j.earscirev.2015.09.011 (2016).
74 Herman, F., De Doncker, F., Delaney, I., Prasicek, G. & Koppes, M. The impact of glaciers on mountain erosion. *Nature Reviews Earth & Environment* **2**, 422-435, doi:10.1038/s43017-021-00165-9 (2021).
75 Antoniazza, G. & Lane, S. N. Sediment yield over glacial cycles: A conceptual model. *Progress in Physical Geography: Earth and Environment*, doi:10.1177/0309133321997292 (2021).
76 Hallet, B., Hunter, L. & Bogen, J. Rates of erosion and sediment evacuation by glaciers: A review of field data and their implications. *Global and Planetary Change* **12**, 213-235, doi:https://doi.org/10.1016/0921-8181(95)00021-6 (1996).
77 Cook, S. J., Swift, D. A., Kirkbride, M. P., Knight, P. G. & Waller, R. I. The empirical basis for modelling glacial erosion rates. *Nat Commun* **11**, 759, doi:10.1038/s41467-020-14583-8 (2020).
78 Ugelvig, S. V., Egholm, D. L., Anderson, R. S. & Iverson, N. R. Glacial Erosion Driven by Variations in

Meltwater Drainage. *Journal of Geophysical Research: Earth Surface* **123**, 2863-2877, doi:10.1029/2018jf004680 (2018).

79 Iverson, N. R. A theory of glacial quarrying for landscape evolution models. *Geology* **40**, 679-682, doi:10.1130/g33079.1 (2012).

80 Hallet, B. Glacial quarrying: a simple theoretical model. *Annals of Glaciology* **22**, 1-8, doi:10.3189/1996AoG22-1-1-8 (1996).

81 Dühnforth, M., Anderson, R. S., Ward, D. & Stock, G. M. Bedrock fracture control of glacial erosion processes and rates. *Geology* **38**, 423-426, doi:10.1130/g30576.1 (2010).

82 Bernard, H. A Theoretical Model of Glacial Abrasion. *JGlac* **23**, 39-50, doi:10.3189/S0022143000029725 (1979).

83 Iverson, N. R. Laboratory Simulations Of Glacial Abrasion: Comparison With Theory. *JGlac* **36**, 304-314, doi:10.3189/002214390793701264 (1990).

84 Harbor, J. M., Hallet, B. & Raymond, C. F. A numerical model of landform development by glacial erosion. *Nature* **333**, 347-349, doi:10.1038/333347a0 (1988).

85 MacGregor, J. A. *et al.* A synthesis of the basal thermal state of the Greenland Ice Sheet. *J Geophys Res Earth Surf* **121**, 1328-1350, doi:10.1002/2015JF003803 (2016).

86 Dehecq, A. *et al.* Twenty-first century glacier slowdown driven by mass loss in High Mountain Asia. *Nature Geoscience* **12**, 22-27, doi:10.1038/s41561-018-0271-9 (2018).

87 Phillips, T., Rajaram, H. & Steffen, K. Cryo-hydrologic warming: A potential mechanism for rapid thermal response of ice sheets. *Geophysical Research Letters* **37**, n/a-n/a, doi:10.1029/2010gl044397 (2010).

88 Carrivick, J. L. & Tweed, F. S. Deglaciation controls on sediment yield: Towards capturing spatio-temporal variability. *Earth-Sci. Rev.* **221**, doi:10.1016/j.earscirev.2021.103809 (2021).

89 Herman, F., Beaud, F., Champagnac, J.-D., Lemieux, J.-M. & Sternai, P. Glacial hydrology and erosion patterns: A mechanism for carving glacial valleys. *Earth and Planetary Science Letters* **310**, 498-508, doi:10.1016/j.epsl.2011.08.022 (2011).

90 Alley, R. B. *et al.* How glaciers entrain and transport basal sediment: Physical constraints. *QSRv* **16**, 1017-1038, doi:https://doi.org/10.1016/S0277-3791(97)00034-6 (1997).

91 Hartmeyer, I. *et al.* Current glacier recession causes significant rockfall increase: the immediate paraglacial response of deglaciating cirque walls. *Earth Surface Dynamics* **8**, 729-751, doi:10.5194/esurf-8-729-2020 (2020).

92 Coe, J. A., Bessette-Kirton, E. K. & Geertsema, M. Increasing rock-avalanche size and mobility in Glacier Bay National Park and Preserve, Alaska detected from 1984 to 2016 Landsat imagery. *Landslides* **15**, 393-407, doi:10.1007/s10346-017-0879-7 (2017).

93 Beylich, A. A. & Laute, K. Sediment sources, spatiotemporal variability and rates of fluvial bedload transport in glacier-connected steep mountain valleys in western Norway (Erdalen and Bødalen drainage basins). *Geomo* **228**, 552-567, doi:10.1016/j.geomorph.2014.10.018 (2015).

94 Allen, S. K., Cox, S. C. & Owens, I. F. Rock avalanches and other landslides in the central Southern Alps of New Zealand: a regional study considering possible climate change impacts. *Landslides* **8**, 33-48, doi:10.1007/s10346-010-0222-z (2010).

95 Chiarle, M., Geertsema, M., Mortara, G. & Clague, J. J. Relations between climate change and mass movement: Perspectives from the Canadian Cordillera and the European Alps. *Global and Planetary Change* **202**, doi:10.1016/j.gloplacha.2021.103499 (2021).

96 Matsuoka, N. Frost weathering and rockwall erosion in the southeastern Swiss Alps: Long-term (1994–2006) observations. *Geomo* **99**, 353-368, doi:10.1016/j.geomorph.2007.11.013 (2008).

97 Murton, J. B., Peterson, R. & Ozouf, J.-C. Bedrock Fracture by Ice Segregation in Cold Regions. *Science* **314**, 1127-1129, doi:doi:10.1126/science.1132127 (2006).

98 Kellerer-Pirklbauer, A. Potential weathering by freeze-thaw action in alpine rocks in the European Alps during a nine year monitoring period. *Geomo* **296**, 113-131, doi:10.1016/j.geomorph.2017.08.020 (2017).

99 Scherler, D. & Egholm, D. L. Production and Transport of Supraglacial Debris: Insights From Cosmogenic 10Be and Numerical Modeling, Chhota Shigri Glacier, Indian Himalaya. *Journal of Geophysical Research: Earth Surface* **125**, doi:10.1029/2020jf005586 (2020).

100 Evans, S. G. & Delaney, K. B. in *Snow and Ice-Related Hazards, Risks, and Disasters* (eds John F. Shroder, Wilfried Haeberli, & Colin Whiteman) 563-606 (Academic Press, 2015).

101 Beaud, F., Flowers, G. E. & Venditti, J. G. Efficacy of bedrock erosion by subglacial water flow. *Earth Surface Dynamics* **4**, 125-145, doi:10.5194/esurf-4-125-2016 (2016).

102 Gimbert, F., Tsai, V. C., Amundson, J. M., Bartholomaus, T. C. & Walter, J. I. Subseasonal changes observed in subglacial channel pressure, size, and sediment transport. *Geophysical Research Letters* **43**, 3786-3794, doi:10.1002/2016gl068337 (2016).

103 Swift, D. A. *et al.* The hydrology of glacier-bed overdeepenings: Sediment transport mechanics, drainage system morphology, and geomorphological implications. *ESPL* **46**, 2264-2278, doi:10.1002/esp.5173 (2021).

104 Andrews, L. C. *et al.* Direct observations of evolving subglacial drainage beneath the Greenland Ice Sheet. *Nature* **514**, 80-83, doi:10.1038/nature13796 (2014).

105 Colgan, W. *et al.* An increase in crevasse extent, West Greenland: Hydrologic implications. *Geophysical Research Letters* **38**, n/a-n/a, doi:10.1029/2011gl048491 (2011).

106 Nienow, P., Sharp, M. & Willis, I. Seasonal changes in the morphology of the subglacial drainage system, Haut Glacier d'Arolla, Switzerland. *ESPL* **23**, 825-843, doi:https://doi.org/10.1002/(SICI)1096-9837(199809)23:9<825::AID-ESP893>3.0.CO;2-2 (1998).

107 Chudley, T. R. *et al.* Supraglacial lake drainage at a fast-flowing Greenlandic outlet glacier. *Proc Natl Acad Sci U S A* **116**, 25468-25477, doi:10.1073/pnas.1913685116 (2019).

108 Smith, L. C. *et al.* Efficient meltwater drainage through supraglacial streams and rivers on the southwest Greenland ice sheet. *Proc Natl Acad Sci U S A* **112**, 1001-1006, doi:10.1073/pnas.1413024112 (2015).

109 Livingstone, S. J. *et al.* Subglacial lakes and their changing role in a warming climate. *Nature Reviews Earth & Environment*, doi:10.1038/s43017-021-00246-9 (2022).

110 Livingstone, S. J. *et al.* Brief communication: Subglacial lake drainage beneath Isunguata Sermia, West Greenland: geomorphic and ice dynamic effects. *The Cryosphere* **13**, 2789-2796, doi:10.5194/tc-13-2789-2019 (2019).

111 Gabet, E., Burbank, D., Prattsitaula, B., Putkonen, J. & Bookhagen, B. Modern erosion rates in the High Himalayas of Nepal. *Earth and Planetary Science Letters* **267**, 482-494, doi:10.1016/j.epsl.2007.11.059 (2008).

112 Tsyplenkov, A., Vanmaercke, M., Collins, A. L., Kharchenko, S. & Golosov, V. Elucidating suspended sediment dynamics in a glacierized catchment after an exceptional erosion event: The Djankuat catchment, Caucasus Mountains, Russia. *Catena* **203**, doi:10.1016/j.catena.2021.105285 (2021).

113 Beylich, A. A., Laute, K. & Storms, J. E. A. Contemporary suspended sediment dynamics within two partly glacierized mountain drainage basins in western Norway (Erdalen and Bødalen, inner Nordfjord). *Geomo* **287**, 126-143, doi:10.1016/j.geomorph.2015.12.013 (2017).

114 Comiti, F. *et al.* Glacier melt runoff controls bedload transport in Alpine catchments. *Earth and Planetary Science Letters* **520**, 77-86, doi:10.1016/j.epsl.2019.05.031 (2019).

115 Williams, H. B. & Koppes, M. N. A comparison of glacial and paraglacial denudation responses to rapid glacial retreat. *Annals of Glaciology* **60**, 151-164, doi:10.1017/aog.2020.1 (2019).

116 Bogen, J., Xu, M. & Kennie, P. The impact of pro-glacial lakes on downstream sediment delivery in Norway. *ESPL* **40**, 942-952, doi:10.1002/esp.3669 (2014).

117 Steffen, T., Huss, M., Estermann, R., Hodel, E. & Farinotti, D. Volume, evolution, and sedimentation of future glacier lakes in Switzerland over the 21st century. *Earth Surface Dynamics* **10**, 723-741, doi:10.5194/esurf-10-723-2022 (2022).

118 Cook, K. L., Andermann, C., Gimbert, F., Adhikari, B. R. & Hovius, N. Glacial lake outburst floods as drivers of fluvial erosion in the Himalaya. *Science* **362**, 53-57, doi:doi:10.1126/science.aat4981 (2018).

119 Cenderelli, D. A. & Wohl, E. E. Flow hydraulics and geomorphic effects of glacial-lake outburst floods in the Mount Everest region, Nepal. *ESPL* **28**, 385-407, doi:10.1002/esp.448 (2003).

120 Heckmann, T., McColl, S. & Morche, D. Retreating ice: research in pro-glacial areas matters. *ESPL* **41**, 271-276, doi:10.1002/esp.3858 (2016).

121 Tomczyk, A. M., Ewertowski, M. W. & Carrivick, J. L. Geomorphological impacts of a glacier lake outburst flood in the high arctic Zackenberg River, NE Greenland. *Journal of Hydrology* **591**, doi:10.1016/j.jhydrol.2020.125300 (2020).

122 Russell, A. J. *et al.* Icelandic jökulhlaup impacts: Implications for ice-sheet hydrology, sediment transfer and geomorphology. *Geomo* **75**, 33-64, doi:10.1016/j.geomorph.2005.05.018 (2006).

123 Wilson, R. *et al.* The 2015 Chileno Valley glacial lake outburst flood, Patagonia. *Geomo* **332**, 51-65, doi:10.1016/j.geomorph.2019.01.015 (2019).

124 IPCC. Climate Change 2021: The Physical Science Basis. Contribution of Working Group I to the Sixth Assessment Report of the Intergovernmental Panel on Climate Change. (Cambridge University Press, 2021).

125 de Winter, I. L., Storms, J. E. A. & Overeem, I. Numerical modeling of glacial sediment production and transport during deglaciation. *Geomo* **167-168**, 102-114, doi:10.1016/j.geomorph.2012.05.023 (2012).

126 Lai, J. & Anders, A. M. Climatic controls on mountain glacier basal thermal regimes dictate spatial patterns of glacial erosion. *Earth Surface Dynamics* **9**, 845-859, doi:10.5194/esurf-9-845-2021 (2021).

127 Hirschberg, J. *et al.* Climate Change Impacts on Sediment Yield and Debris-Flow Activity in an Alpine Catchment. *Journal of Geophysical Research: Earth Surface* **126**, e2020JF005739, doi:https://doi.org/10.1029/2020JF005739 (2021).

128 Kokelj, S. V. *et al.* Thawing of massive ground ice in mega slumps drives increases in stream sediment and solute flux across a range of watershed scales. *Journal of Geophysical Research: Earth Surface* **118**, 681-692, doi:10.1002/jgrf.20063 (2013).

129 Rudy, A. C. A., Lamoureux, S. F., Kokelj, S. V., Smith, I. R. & England, J. H. Accelerating Thermokarst Transforms Ice-Cored Terrain Triggering a Downstream Cascade to the Ocean. *Geophysical Research Letters* **44**, doi:10.1002/2017gl074912 (2017).

130 Lafrenière, M. J. & Lamoureux, S. F. Effects of changing permafrost conditions on hydrological processes and fluvial fluxes. *Earth-Sci. Rev.* **191**, 212-223, doi:10.1016/j.earscirev.2019.02.018 (2019).

131 Lamoureux, S. F., Lafrenière, M. J. & Favaro, E. A. Erosion dynamics following localized permafrost slope disturbances. *Geophysical Research Letters* **41**, 5499-5505, doi:10.1002/2014gl060677 (2014).

132 Godin, E., Fortier, D. & Coulombe, S. Effects of thermo-erosion gullying on hydrologic flow networks, discharge and soil loss. *Environmental Research Letters* **9**, 105010, doi:10.1088/1748-9326/9/10/105010 (2014).

133 Obu, J. *et al.* Effect of Terrain Characteristics on Soil Organic Carbon and Total Nitrogen Stocks in Soils of Herschel Island, Western Canadian Arctic. *Permafrost and Periglacial Processes* **28**, 92-107,

doi:https://doi.org/10.1002/ppp.1881 (2017).

134 Lewkowicz, A. G. Dynamics of active-layer detachment failures, Fosheim Peninsula, Ellesmere Island, Nunavut, Canada. *Permafrost and Periglacial Processes* **18**, 89-103, doi:10.1002/ppp.578 (2007).

135 Gooseff, M. N., Balser, A., Bowden, W. B. & Jones, J. B. Effects of Hillslope Thermokarst in Northern Alaska. *Eos, Transactions American Geophysical Union* **90**, 29-30, doi:https://doi.org/10.1029/2009EO040001 (2009).

136 Paquette, M., Rudy, A. C. A., Fortier, D. & Lamoureux, S. F. Multi-scale site evaluation of a relict active layer detachment in a High Arctic landscape. *Geomo* **359**, doi:10.1016/j.geomorph.2020.107159 (2020).

137 Balser, A. W., Jones, J. B. & Gens, R. Timing of retrogressive thaw slump initiation in the Noatak Basin, northwest Alaska, USA. *Journal of Geophysical Research: Earth Surface* **119**, 1106-1120, doi:10.1002/2013jf002889 (2014).

138 Godin, E. & Fortier, D. Geomorphology of a thermo-erosion gully, Bylot Island, Nunavut, Canada. *CaJES* **49**, 979-986, doi:10.1139/e2012-015 (2012).

139 Perreault, N., Lévesque, E., Fortier, D., Gratton, D. & Lamarque, L. J. Remote sensing evaluation of High Arctic wetland depletion following permafrost disturbance by thermo-erosion gullying processes. *Arctic Science* **3**, 237-253, doi:10.1139/as-2016-0047 (2017).

140 Kokelj, S. V. *et al.* Thaw-driven mass wasting couples slopes with downstream systems, and effects propagate through Arctic drainage networks. *The Cryosphere* **15**, 3059-3081, doi:10.5194/tc-15-3059-2021 (2021).

141 Zheng, L., Overeem, I., Wang, K. & Clow, G. D. Changing Arctic River Dynamics Cause Localized Permafrost Thaw. *Journal of Geophysical Research: Earth Surface* **124**, 2324-2344, doi:10.1029/2019jf005060 (2019).

142 Lantuit, H. & Pollard, W. H. Fifty years of coastal erosion and retrogressive thaw slump activity on Herschel Island, southern Beaufort Sea, Yukon Territory, Canada. *Geomo* **95**, 84-102, doi:10.1016/j.geomorph.2006.07.040 (2008).

143 Costard, F., Dupeyrat, L., Gautier, E. & Carey-Gailhardis, E. Fluvial thermal erosion investigations along a rapidly eroding river bank: application to the Lena River (central Siberia). *ESPL* **28**, 1349-1359, doi:10.1002/esp.592 (2003).

144 Payne, C., Panda, S. & Prakash, A. Remote Sensing of River Erosion on the Colville River, North Slope Alaska. *Remote Sensing* **10**, doi:10.3390/rs10030397 (2018).

145 Costard, F. *et al.* Impact of the global warming on the fluvial thermal erosion over the Lena River in Central Siberia. *Geophysical Research Letters* **34**, doi:10.1029/2007gl030212 (2007).

146 Gautier, E. *et al.* Fifty-year dynamics of the Lena River islands (Russia): Spatio-temporal pattern of large periglacial anabranching river and influence of climate change. *Sci Total Environ* **783**, 147020, doi:10.1016/j.scitotenv.2021.147020 (2021).

147 Shur, Y. *et al.* Fluvio-thermal erosion and thermal denudation in the yedoma region of northern Alaska: Revisiting the Itkillik River exposure. *Permafrost and Periglacial Processes* **32**, 277-298, doi:10.1002/ppp.2105 (2021).

148 Chassiot, L., Lajeunesse, P. & Bernier, J.-F. Riverbank erosion in cold environments: Review and outlook. *Earth-Sci. Rev.* **207**, doi:10.1016/j.earscirev.2020.103231 (2020).

149 Vandermause, R., Harvey, M., Zevenbergen, L. & Ettema, R. River-ice effects on bank erosion along the middle segment of the Susitna river, Alaska. *Cold Regions Science and Technology* **185**, doi:10.1016/j.coldregions.2021.103239 (2021).

150 Costard, F., Gautier, E., Fedorov, A., Konstantinov, P. & Dupeyrat, L. An Assessment of the Erosion Potential of the Fluvial Thermal Process during Ice Breakups of the Lena River (Siberia). *Permafrost and Periglacial*

Processes **25**, 162-171, doi:10.1002/ppp.1812 (2014).

151 Beltaos, S., Carter, T., Rowsell, R. & DePalma, S. G. S. Erosion potential of dynamic ice breakup in Lower Athabasca River. Part I: Field measurements and initial quantification. *Cold Regions Science and Technology* **149**, 16-28, doi:10.1016/j.coldregions.2018.01.013 (2018).

152 Rowland, J. C. *et al.* Arctic Landscapes in Transition: Responses to Thawing Permafrost. *Eos, Transactions American Geophysical Union* **91**, 229-230, doi:https://doi.org/10.1029/2010EO260001 (2010).

153 Wohl, E. *et al.* Connectivity as an emergent property of geomorphic systems. *ESPL* **44**, 4-26, doi:10.1002/esp.4434 (2019).

154 Walvoord, M. A. & Kurylyk, B. L. Hydrologic Impacts of Thawing Permafrost-A Review. *Vadose Zone Journal* **15**, 1-20 vzj2016.2001.0010, doi:10.2136/vzj2016.01.0010 (2016).

155 Zhang, T., Li, D. & Lu, X. Response of runoff components to climate change in the source-region of the Yellow River on the Tibetan plateau. *Hydrological Processes* **36**, doi:10.1002/hyp.14633 (2022).

156 Farquharson, L. M., Romanovsky, V. E., Kholodov, A. & Nicolsky, D. Sub-aerial talik formation observed across the discontinuous permafrost zone of Alaska. *Nature Geoscience* **15**, 475-481, doi:10.1038/s41561-022-00952-z (2022).

157 Nitzbon, J. *et al.* Fast response of cold ice-rich permafrost in northeast Siberia to a warming climate. *Nat Commun* **11**, 2201, doi:10.1038/s41467-020-15725-8 (2020).

158 Jones, B. M. *et al.* Arctic Report Card 2020: Coastal Permafrost Erosion. doi:https://doi.org/10.25923/e47w-dw52 (2020).

159 Günther, F., Overduin, P. P., Sandakov, A. V., Grosse, G. & Grigoriev, M. N. Short- and long-term thermo-erosion of ice-rich permafrost coasts in the Laptev Sea region. *Biogeosciences* **10**, 4297-4318, doi:10.5194/bg-10-4297-2013 (2013).

160 Lim, M. *et al.* Massive Ice Control on Permafrost Coast Erosion and Sensitivity. *Geophysical Research Letters* **47**, doi:10.1029/2020gl087917 (2020).

161 Frederick, J. M., Thomas, M. A., Bull, D. L., Jones, C. A. & Roberts, J. D. The Arctic coastal erosion problem. *Albuquerque, NM: Sandia National Laboratories SAND2016-9762* **122** (2016).

162 Overeem, I. *et al.* Sea ice loss enhances wave action at the Arctic coast. *Geophysical Research Letters* **38**, L17503, doi:10.1029/2011gl048681 (2011).

163 Radosavljevic, B. *et al.* Erosion and Flooding—Threats to Coastal Infrastructure in the Arctic: A Case Study from Herschel Island, Yukon Territory, Canada. *Estuaries and Coasts* **39**, 900-915, doi:10.1007/s12237-015-0046-0 (2015).

164 Couture, N. J., Irrgang, A., Pollard, W., Lantuit, H. & Fritz, M. Coastal Erosion of Permafrost Soils Along the Yukon Coastal Plain and Fluxes of Organic Carbon to the Canadian Beaufort Sea. *Journal of Geophysical Research: Biogeosciences* **123**, 406-422, doi:10.1002/2017jg004166 (2018).

165 Delaney, I., Bauder, A., Werder, M. A. & Farinotti, D. Regional and Annual Variability in Subglacial Sediment Transport by Water for Two Glaciers in the Swiss Alps. *Frontiers in Earth Science* **6**, doi:10.3389/feart.2018.00175 (2018).

166 Comte, J., Monier, A., Crevecoeur, S., Lovejoy, C. & Vincent, W. F. Microbial biogeography of permafrost thaw ponds across the changing northern landscape. *Ecography* **39**, 609-618, doi:10.1111/ecog.01667 (2016).

167 Fuchs, M. *et al.* Rapid Fluvio-Thermal Erosion of a Yedoma Permafrost Cliff in the Lena River Delta. *Frontiers in Earth Science* **8**, doi:10.3389/feart.2020.00336 (2020).

168 Li, D., Li, Z., Zhou, Y. & Lu, X. Substantial Increases in the Water and Sediment Fluxes in the Headwater Region of the Tibetan Plateau in Response to Global Warming. *Geophysical Research Letters* **47**,

e2020GL087745, doi:https://doi.org/10.1029/2020GL087745 (2020).
169 Zhang, F. *et al.* Controls on seasonal erosion behavior and potential increase in sediment evacuation in the warming Tibetan Plateau. *Catena* **209**, doi:10.1016/j.catena.2021.105797 (2022).
170 Singh, A. *et al.* Counter-intuitive influence of Himalayan river morphodynamics on Indus Civilisation urban settlements. *Nat Commun* **8**, 1617, doi:10.1038/s41467-017-01643-9 (2017).
171 Gabbud, C., Robinson, C. T. & Lane, S. N. Summer is in winter: Disturbance-driven shifts in macroinvertebrate communities following hydroelectric power exploitation. *Sci Total Environ* **650**, 2164-2180, doi:10.1016/j.scitotenv.2018.09.180 (2019).
172 Fischer, L., Huggel, C., Kääb, A. & Haeberli, W. Slope failures and erosion rates on a glacierized high-mountain face under climatic changes. *ESPL* **38**, 836-846, doi:10.1002/esp.3355 (2013).
173 Bogen, J. The impact of climate change on glacial sediment delivery to rivers. *IAHS-AISH publ* **325**, 432-439 (2008).
174 Singh, A. T. *et al.* Water discharge and suspended sediment dynamics in the Chandra River, Western Himalaya. *Journal of Earth System Science* **129**, doi:10.1007/s12040-020-01455-4 (2020).
175 Brooke, S. *et al.* Where rivers jump course. *Science* **376**, 987-990, doi:doi:10.1126/science.abm1215 (2022).
176 Church, M. & Ryder, J. M. Paraglacial Sedimentation: A Consideration of Fluvial Processes Conditioned by Glaciation. *GSA Bulletin* **83**, 3059-3072, doi:10.1130/0016-7606(1972)83[3059:Psacof]2.0.Co;2 (1972).
177 Ballantyne, C. K. Paraglacial geomorphology. *QSRv* **21**, 1935-2017, doi:https://doi.org/10.1016/S0277-3791(02)00005-7 (2002).
178 Mariotti, A. *et al.* Nonlinear forcing of climate on mountain denudation during glaciations. *Nature Geoscience*, doi:10.1038/s41561-020-00672-2 (2021).
179 Moon, S. *et al.* Climatic control of denudation in the deglaciated landscape of the Washington Cascades. *Nature Geoscience* **4**, 469-473, doi:10.1038/ngeo1159 (2011).
180 Terhaar, J., Lauerwald, R., Regnier, P., Gruber, N. & Bopp, L. Around one third of current Arctic Ocean primary production sustained by rivers and coastal erosion. *Nat Commun* **12**, 169, doi:10.1038/s41467-020-20470-z (2021).
181 Ogorodov, S., Aleksyutina, D., Baranskaya, A., Shabanova, N. & Shilova, O. Coastal Erosion of the Russian Arctic: An Overview. *J. Coast. Res.* **95**, 599-604, doi:10.2112/si95-117.1 (2020).
182 Guégan, E. *Erosion of permafrost affected coasts: rates, mechanisms and modelling* PhD thesis, NTNU, (2015).
183 Jones, B. M. *et al.* Increase in the rate and uniformity of coastline erosion in Arctic Alaska. *Geophysical Research Letters* **36**, L03503, doi:10.1029/2008gl036205 (2009).
184 Hasholt, B., van As, D., Mikkelsen, A. B., Mernild, S. H. & Yde, J. C. Observed sediment and solute transport from the Kangerlussuaq sector of the Greenland Ice Sheet (2006–2016). *Arct. Antarct. Alp. Res.* **50**, doi:10.1080/15230430.2018.1433789 (2018).
185 Hudson, B. *et al.* MODIS observed increase in duration and spatial extent of sediment plumes in Greenland fjords. *The Cryosphere* **8**, 1161-1176, doi:10.5194/tc-8-1161-2014 (2014).
186 Overeem, I., Nienhuis, J. H. & Piliouras, A. Ice-dominated Arctic deltas. *Nature Reviews Earth & Environment*, doi:10.1038/s43017-022-00268-x (2022).
187 Fritz, M., Vonk, J. E. & Lantuit, H. Collapsing Arctic coastlines. *Nature Climate Change* **7**, 6-7, doi:10.1038/nclimate3188 (2017).
188 Huss, M. *et al.* Toward mountains without permanent snow and ice. *Earth's Future* **5**, 418-435, doi:10.1002/2016ef000514 (2017).
189 Schaefer, K., Zhang, T., Bruhwiler, L. & Barrett, A. P. Amount and timing of permafrost carbon release in

response to climate warming. *Tellus B* **63**, 165-180, doi:10.1111/j.1600-0889.2011.00527.x (2011).

190 Sadai, S., Condron, A., DeConto, R. & Pollard, D. Future climate response to Antarctic Ice Sheet melt caused by anthropogenic warming. *Science Advances* **6**, eaaz1169, doi:doi:10.1126/sciadv.aaz1169 (2020).

191 Aschwanden, A. *et al.* Contribution of the Greenland Ice Sheet to sea level over the next millennium. *Science Advances* **5**, eaav9396, doi:doi:10.1126/sciadv.aav9396 (2019).

192 Knight, J. & Harrison, S. Mountain glacial and paraglacial environments under global climate change: lessons from the past, future directions and policy implications. *Geogr. Ann. Ser. A-Phys. Geogr.* **96**, 245-264, doi:10.1111/geoa.12051 (2014).

193 Costa, A. *et al.* Temperature signal in suspended sediment export from an Alpine catchment. *HESS* **22**, 509-528, doi:10.5194/hess-22-509-2018 (2018).

194 Church, M. & Slaymaker, O. Disequilibrium of Holocene sediment yield in glaciated British Columbia. *Nature* **337**, 452-454, doi:10.1038/337452a0 (1989).

195 Slosson, J. R., Kelleher, C. & Hoke, G. D. Contrasting Impacts of a Hotter and Drier Future on Streamflow and Catchment Scale Sediment Flux in the High Andes. *Journal of Geophysical Research: Earth Surface* **126**, doi:10.1029/2021jf006182 (2021).

196 Walling, D. E. Human impact on land–ocean sediment transfer by the world's rivers. *Geomo* **79**, 192-216, doi:10.1016/j.geomorph.2006.06.019 (2006).

197 Li, L. *et al.* Global trends in water and sediment fluxes of the world's large rivers. *Science Bulletin* **65**, 62-69, doi:10.1016/j.scib.2019.09.012 (2020).

198 Pandey, A., Himanshu, S. K., Mishra, S. K. & Singh, V. P. Physically based soil erosion and sediment yield models revisited. *Catena* **147**, 595-620, doi:10.1016/j.catena.2016.08.002 (2016).

199 de Vente, J. *et al.* Predicting soil erosion and sediment yield at regional scales: Where do we stand? *Earth-Sci. Rev.* **127**, 16-29, doi:10.1016/j.earscirev.2013.08.014 (2013).

200 Walling, D. E. The sediment delivery problem. *Journal of Hydrology* **65**, 209-237, doi:https://doi.org/10.1016/0022-1694(83)90217-2 (1983).

201 Vercruysse, K., Grabowski, R. C. & Rickson, R. J. Suspended sediment transport dynamics in rivers: Multi-scale drivers of temporal variation. *Earth-Sci. Rev.* **166**, 38-52, doi:10.1016/j.earscirev.2016.12.016 (2017).

202 Harrison, S. *et al.* Uncertainty in geomorphological responses to climate change. *Climatic Change* **156**, 69-86, doi:10.1007/s10584-019-02520-8 (2019).

203 Qin, D. & Ding, Y. Key Issues on Cryospheric Changes, Trends and Their Impacts. *Advances in Climate Change Research* **1**, 1-10, doi:10.3724/sp.J.1248.2010.00001 (2010).

204 Thackeray, C. W. & Hall, A. An emergent constraint on future Arctic sea-ice albedo feedback. *Nature Climate Change* **9**, 972-978, doi:10.1038/s41558-019-0619-1 (2019).

205 Fang, H.-W. & Wang, G.-Q. Three-dimensional mathematical model of suspended-sediment transport. *Journal of Hydraulic Engineering* **126**, 578-592 (2000).

206 Syvitski, James P. M. & Milliman, John D. Geology, Geography, and Humans Battle for Dominance over the Delivery of Fluvial Sediment to the Coastal Ocean. *The Journal of Geology* **115**, 1-19, doi:10.1086/509246 (2007).

207 Koppes, M. N. & Montgomery, D. R. The relative efficacy of fluvial and glacial erosion over modern to orogenic timescales. *Nature Geoscience* **2**, 644-647, doi:10.1038/ngeo616 (2009).

208 Hinderer, M., Kastowski, M., Kamelger, A., Bartolini, C. & Schlunegger, F. River loads and modern denudation of the Alps — A review. *Earth-Sci. Rev.* **118**, 11-44, doi:10.1016/j.earscirev.2013.01.001 (2013).

209 Wolman, M. G. & Miller, J. P. Magnitude and Frequency of Forces in Geomorphic Processes. *The Journal of Geology* **68**, 54-74, doi:10.1086/626637 (1960).

210 Gariano, S. L. & Guzzetti, F. Landslides in a changing climate. *Earth-Sci. Rev.* **162**, 227-252, doi:10.1016/j.earscirev.2016.08.011 (2016).

211 McMillan, S. K. *et al.* Before the storm: antecedent conditions as regulators of hydrologic and biogeochemical response to extreme climate events. *Biogeochemistry* **141**, 487-501, doi:10.1007/s10533-018-0482-6 (2018).

212 Schumm, S. A. Geomorphic Thresholds: The Concept and Its Applications. *Transactions of the Institute of British Geographers* **4**, 485-515, doi:10.2307/622211 (1979).

213 Phillips, J. D. Evolutionary geomorphology: thresholds and nonlinearity in landform response to environmental change. *Hydrol. Earth Syst. Sci.* **10**, 731-742, doi:10.5194/hess-10-731-2006 (2006).

214 Katzenberger, A., Schewe, J., Pongratz, J. & Levermann, A. Robust increase of Indian monsoon rainfall and its variability under future warming in CMIP6 models. *Earth System Dynamics* **12**, 367-386, doi:10.5194/esd-12-367-2021 (2021).

215 Rao, M. P. *et al.* Seven centuries of reconstructed Brahmaputra River discharge demonstrate underestimated high discharge and flood hazard frequency. *Nat Commun* **11**, 6017, doi:10.1038/s41467-020-19795-6 (2020).

216 Heckmann, T. *et al.* Indices of sediment connectivity: opportunities, challenges and limitations. *Earth-Sci. Rev.* **187**, 77-108, doi:10.1016/j.earscirev.2018.08.004 (2018).

217 Syvitski, J. P. M., Vörösmarty, C. J., Kettner, A. J. & Green, P. Impact of Humans on the Flux of Terrestrial Sediment to the Global Coastal Ocean. *Science* **308**, 376, doi:10.1126/science.1109454 (2005).

218 Piliouras, A. & Rowland, J. C. Arctic River Delta Morphologic Variability and Implications for Riverine Fluxes to the Coast. *Journal of Geophysical Research: Earth Surface* **125**, doi:10.1029/2019jf005250 (2020).

219 Valenza, J. M., Edmonds, D. A., Hwang, T. & Roy, S. Downstream changes in river avulsion style are related to channel morphology. *Nat Commun* **11**, 2116, doi:10.1038/s41467-020-15859-9 (2020).

220 Liu, K. *et al.* Ongoing Drainage Reorganization Driven by Rapid Lake Growths on the Tibetan Plateau. *Geophysical Research Letters* **48**, doi:10.1029/2021gl095795 (2021).

221 Richardson, P. W., Perron, J. T. & Schurr, N. D. Influences of climate and life on hillslope sediment transport. *Geology* **47**, 423-426, doi:10.1130/g45305.1 (2019).

222 Zhou, Y. *et al.* Distinguishing the multiple controls on the decreased sediment flux in the Jialing River basin of the Yangtze River, Southwestern China. *Catena* **193**, doi:10.1016/j.catena.2020.104593 (2020).

223 Zhang, S., Fan, W., Li, Y. & Yi, Y. The influence of changes in land use and landscape patterns on soil erosion in a watershed. *Sci Total Environ* **574**, 34-45, doi:10.1016/j.scitotenv.2016.09.024 (2017).

224 Zhu, Z. *et al.* Greening of the Earth and its drivers. *Nature Climate Change* **6**, 791-795, doi:10.1038/nclimate3004 (2016).

225 Miao, C., Ni, J., Borthwick, A. G. L. & Yang, L. A preliminary estimate of human and natural contributions to the changes in water discharge and sediment load in the Yellow River. *Global and Planetary Change* **76**, 196-205, doi:10.1016/j.gloplacha.2011.01.008 (2011).

226 Mouyen, M. *et al.* Assessing modern river sediment discharge to the ocean using satellite gravimetry. *Nat Commun* **9**, 3384, doi:10.1038/s41467-018-05921-y (2018).

227 Dethier, E. N., Renshaw, C. E. & Magilligan, F. J. Rapid changes to global river suspended sediment flux by humans. *Science* **376**, 1447-1452, doi:doi:10.1126/science.abn7980 (2022).

228 Huntley, D. *et al.* Field testing innovative differential geospatial and photogrammetric monitoring technologies in mountainous terrain near Ashcroft, British Columbia, Canada. *J Mt Sci* **18**, 1-20, doi:10.1007/s11629-020-6552-y (2021).

229 Piret, L. *et al.* High-resolution fjord sediment record of a receding glacier with growing intermediate

proglacial lake (Steffen Fjord, Chilean Patagonia). *ESPL* **46**, 239-251, doi:10.1002/esp.5015 (2020).

230 Deino, A. L. *et al.* Chronostratigraphic model of a high-resolution drill core record of the past million years from the Koora Basin, south Kenya Rift: Overcoming the difficulties of variable sedimentation rate and hiatuses. *QSRv* **215**, 213-231, doi:10.1016/j.quascirev.2019.05.009 (2019).

231 Cook, K. L. *et al.* Detection and potential early warning of catastrophic flow events with regional seismic networks. *Science* **374**, 87-92, doi:doi:10.1126/science.abj1227 (2021).

232 Cohen, S., Kettner, A. J., Syvitski, J. P. M. & Fekete, B. M. WBMsed, a distributed global-scale riverine sediment flux model: Model description and validation. *Computers & Geosciences* **53**, 80-93, doi:10.1016/j.cageo.2011.08.011 (2013).

233 Kettner, A. J. & Syvitski, J. P. M. HydroTrend v.3.0: A climate-driven hydrological transport model that simulates discharge and sediment load leaving a river system. *Computers & Geosciences* **34**, 1170-1183, doi:10.1016/j.cageo.2008.02.008 (2008).

234 Nearing, M. A., Foster, G. R., Lane, L. & Finkner, S. A process-based soil erosion model for USDA-Water Erosion Prediction Project technology. *Trans. ASAE* **32**, 1587-1593 (1989).

235 Reichstein, M. *et al.* Deep learning and process understanding for data-driven Earth system science. *Nature* **566**, 195-204, doi:10.1038/s41586-019-0912-1 (2019).

236 Huang, L., Luo, J., Lin, Z., Niu, F. & Liu, L. Using deep learning to map retrogressive thaw slumps in the Beiluhe region (Tibetan Plateau) from CubeSat images. *Remote Sensing of Environment* **237**, doi:10.1016/j.rse.2019.111534 (2020).

237 Tan, Z., Leung, L. R., Li, H. Y. & Tesfa, T. Modeling Sediment Yield in Land Surface and Earth System Models: Model Comparison, Development, and Evaluation. *Journal of Advances in Modeling Earth Systems* **10**, 2192-2213, doi:10.1029/2017ms001270 (2018).

238 Pfeffer, W. T. *et al.* The Randolph Glacier Inventory: a globally complete inventory of glaciers. *JGlac* **60**, 537-552, doi:10.3189/2014JoG13J176 (2014).

239 Obu, J. *et al.* (NERC EDS Centre for Environmental Data Analysis, NERC EDS Centre for Environmental Data Analysis, 2021).

240 Strauss, J. *et al.* Database of Ice-Rich Yedoma Permafrost (IRYP). *PANGAEA*, doi:10.1594/PANGAEA.861733 (2016).

Acknowledgements

This work was supported by Singapore MOE (A-0003626-00-00; D.L., X.L.), IPCC and Cuomo Foundation (D.L.). The authors acknowledge the valuable comments provided by Michael Church and . We thank Obu Jaroslav, Roger MacLeod, Jérôme Comte, Lingcao Huang, and Wayne Pollard for providing field photos. Any use of trade, firm, or product names is for descriptive purposes only and does not imply endorsement by the U.S. Government.

Author contributions

T.Z. and D.L. conceived the study and assembled the authorship team. T.Z. and D.L. drafted the paper. All authors contributed to the discussion and editing of the manuscript prior to submission.

Competing interests

The authors declare no competing interests.

Peer review information

Nature Reviews Earth & Environment thanks [Referee#1 name], [Referee#2 name] and the other, anonymous, reviewer(s) for their contribution to the peer review of this work.

Publisher's note

Springer Nature remains neutral with regard to jurisdictional claims in published maps and institutional affiliations.

Supplementary information

Supplementary information is available for this paper at https://doi.org/10.1038/s415XX-XXX-XXXX-X

Figure legends

Figure 1. **Glacier melt.** Most of cold regions have experienced rapid glacier mass loss over the past two decades, accompanied by glacial lake expansion and glacial lake outburst floods (GLOFs). Glacier coverage based on the Randolph Glacier Inventory (RGI) 6.0 dataset[238]. Circle color represents glacier elevation change rates (m yr^{-1}) between 2000 and 2019 aggregated for 1°×1° grids within a 90% confidence interval, and circle sizes represent the glacier area[42]. Violet triangles mark locations of recorded GLOFs, with 2,560 GLOF events identified from more than 340 glacial lakes since the 1500s and 1,977 GLOFs occurring after the 1900s[50]. GLOF events triggered by earthquake and geothermal activity have been excluded. Glacial lakes mapped from 2015 to 2018[48] are shown as blue dots.

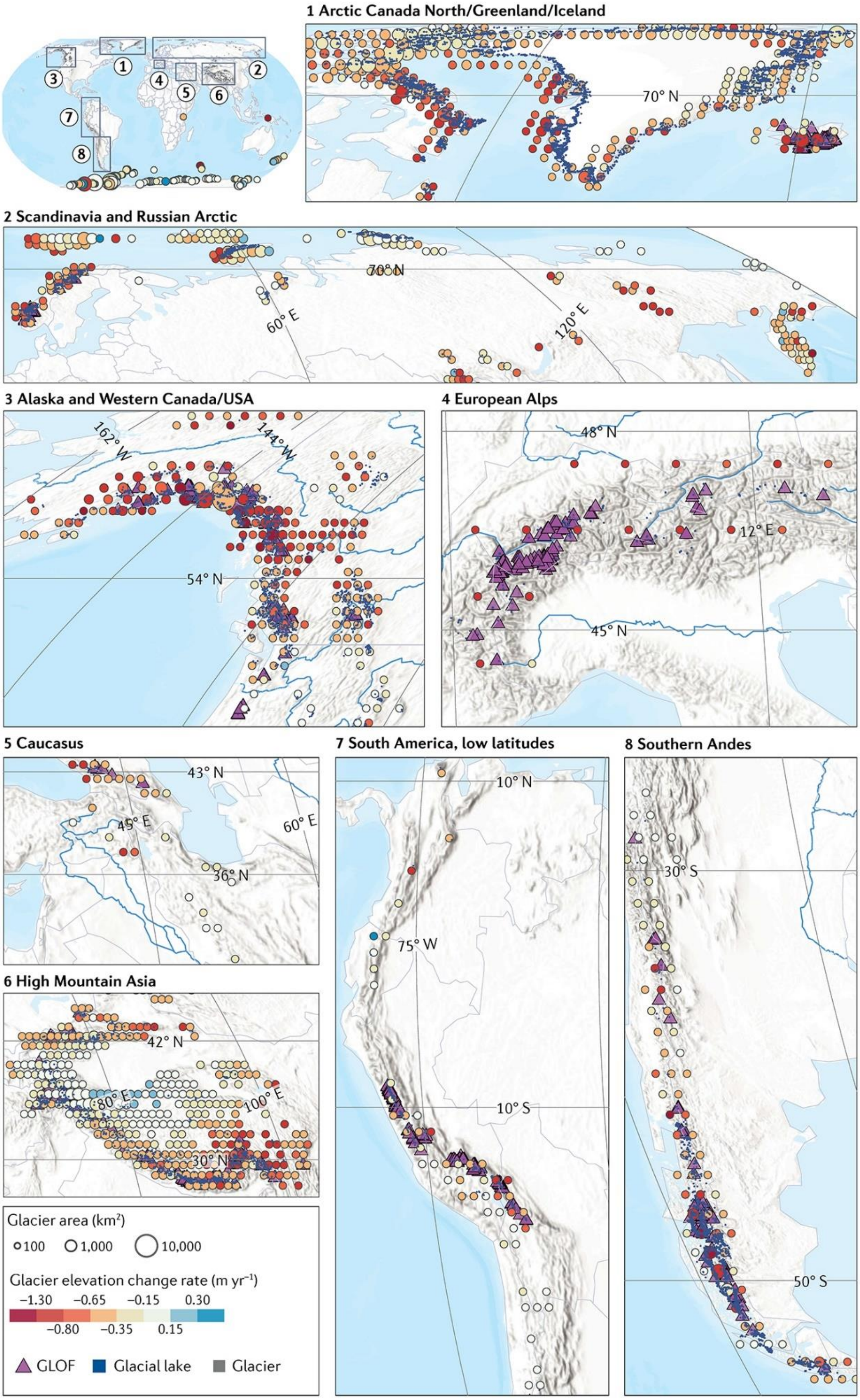
1 Arctic Canada North/Greenland/Iceland
70° N
2 Scandinavia and Russian Arctic
70° N
60° E
120° E
3 Alaska and Western Canada/USA
162° W
144° W
54° N
4 European Alps
48° N
12° E
45° N
5 Caucasus
43° N
45° E
60° E
36° N
6 High Mountain Asia
42° N
80° E
100° E
30° N
7 South America, low latitudes
10° N
75° W
10° S
8 Southern Andes
30° S
50° S
Glacier area (km²)
100
1,000
10,000
Glacier elevation change rate (m yr⁻¹)
−1.30
−0.65
−0.15
0.30
−0.80
−0.35
0.15
GLOF
Glacial lake
Glacier

Figure 2. Permafrost thaw in the Northern Hemisphere. Permafrost has been warming and the active layer has been thickening over the past two decades. Warming trends in mean annual ground temperature (MAGT) near the depth of zero annual amplitude from 2007 to 2016 illustrated by 104 boreholes, drilled to depths of 5-30 m[52]. Deepening of active layer thickness (ALT) over 1997-2019 estimated from the Northern Hemisphere ALT data released by the European Space Agency's Climate Change Initiative Permafrost project[239].The statistical significance (p-value) of ALT change rates is shown in Supplementary Figure 1. Yedoma permafrost is highlighted in violet[240].

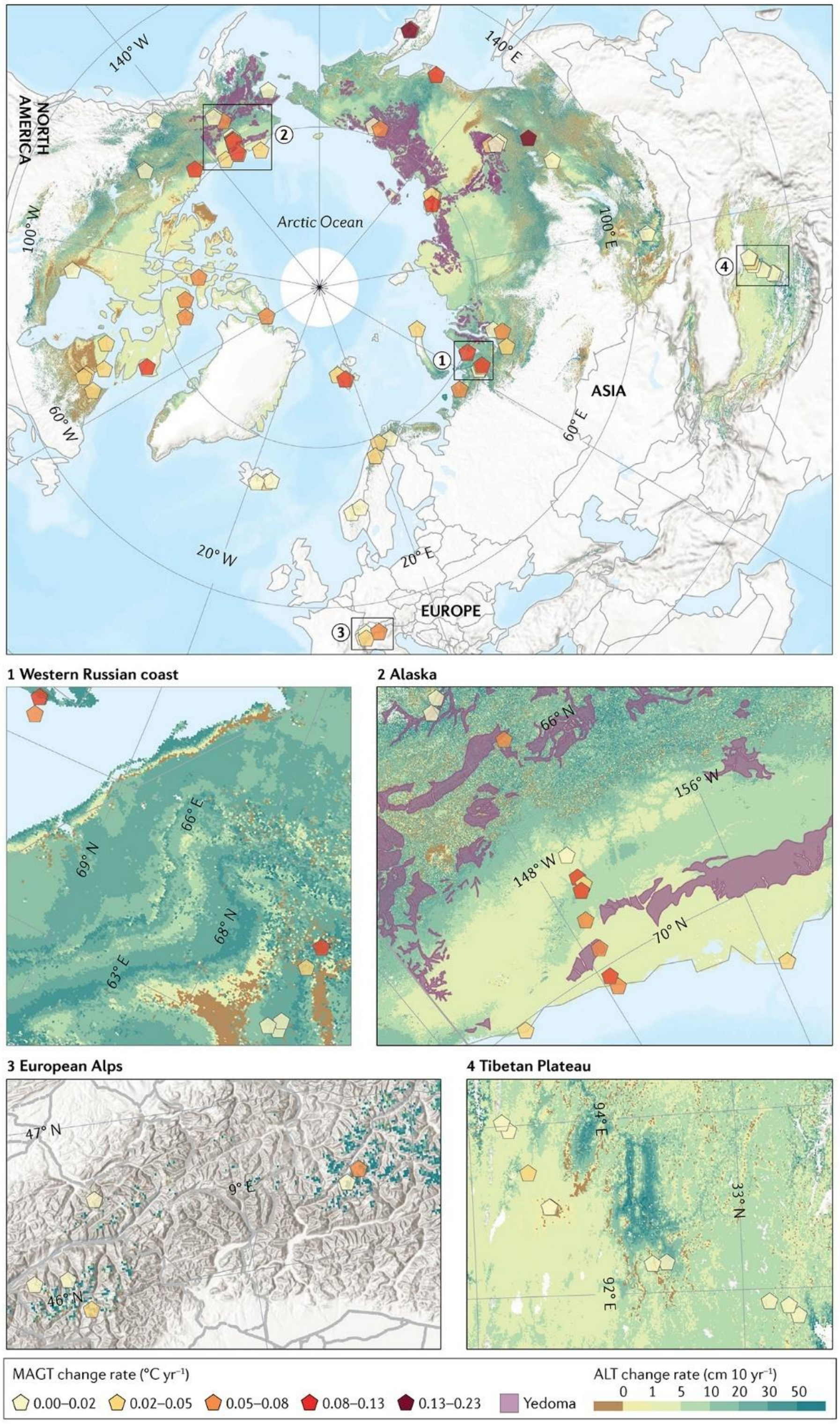

Figure 3. **Impacts of glacier dynamics on sediment transport.** A warming and wetting climate will lead to glacier mass loss, increasing meltwater, erosion and sediment transport initially, followed by an eventual meltwater decline and sediment exhaustion. Positive relationships between variables noted by a + sign, negative relationships by a – sign. Solid blue lines represent small supraglacial channels formed by meltwater or rainfall. Dotted blue lines represent potential englacial channels. Field photos (Numbered 1-9) depict the main glacial erosion processes and features in the diagram.

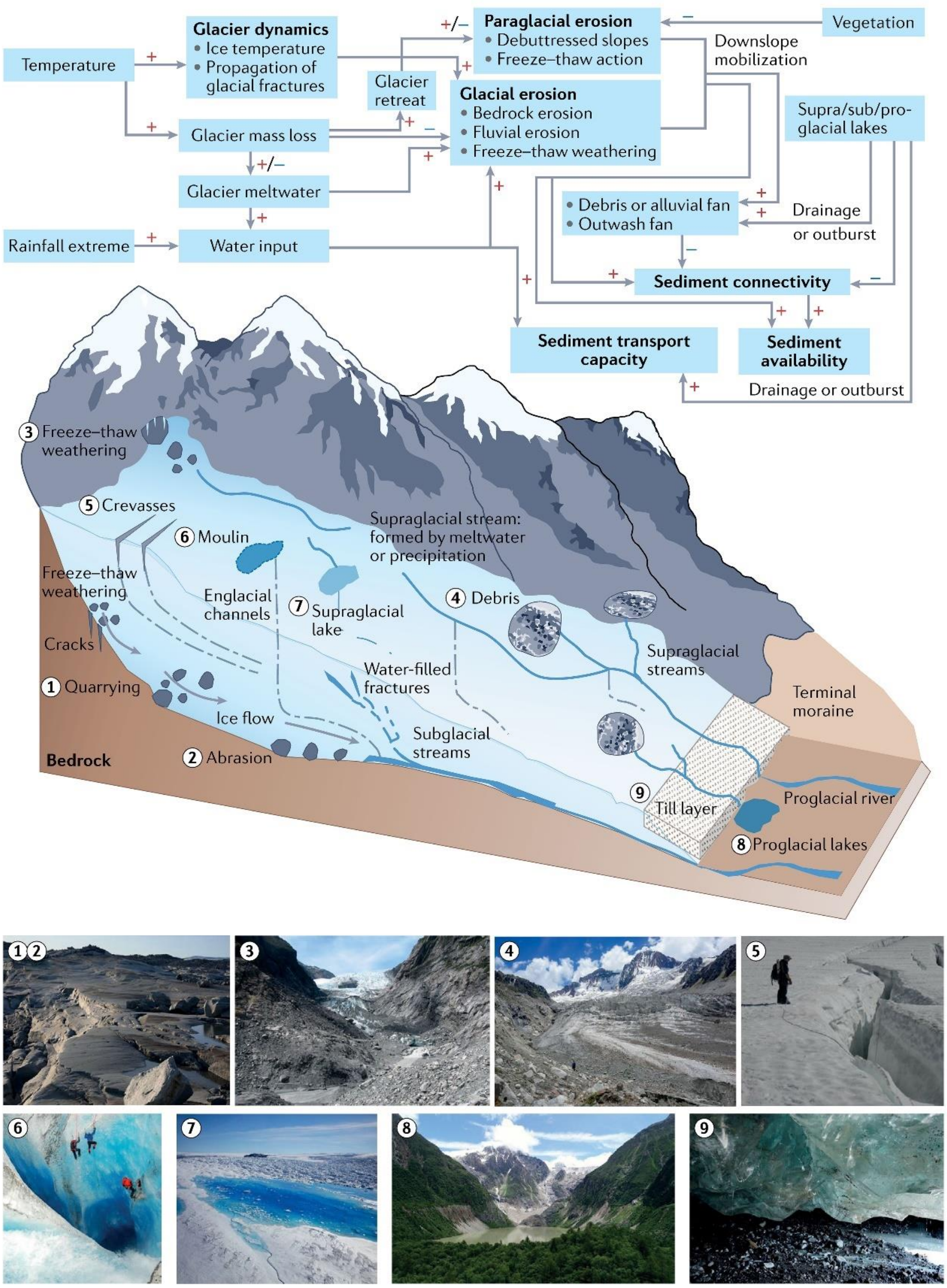

Figure 4. **Impacts of permafrost degradation and thermokarst processes on sediment transport.** Thermokarst processes related to a warming and wetting climate will increase the occurrence of mass movements until the slopes are stabilized. Positive relationships between variables noted by a + sign, negative relationships by a – sign. Field photos (Numbers 1-8) depict key features of thermokarst landscapes and related permafrost erosion processes are depicted in the central panel. Solid blue lines represent the small channels formed by meltwater or rainfall. Dotted blue lines within ice-wedge polygons represent eroded gullies associated with ground ice melting. Brown arrows on thermokarst landscapes mark potential erosion directions. Photos 1–3 courtesy of J. Obu; Photo 4 courtesy of M. Roger/Natural Resources Canada; Photo 5 courtesy of J. Comte/Centre d'études Nordiques; Photo 6 courtesy of B. Richmond/A. Gibbs, U.S. Geological Survey; Photo 7 courtesy of L. Huang; Photo 8 courtesy of W. Pollard.

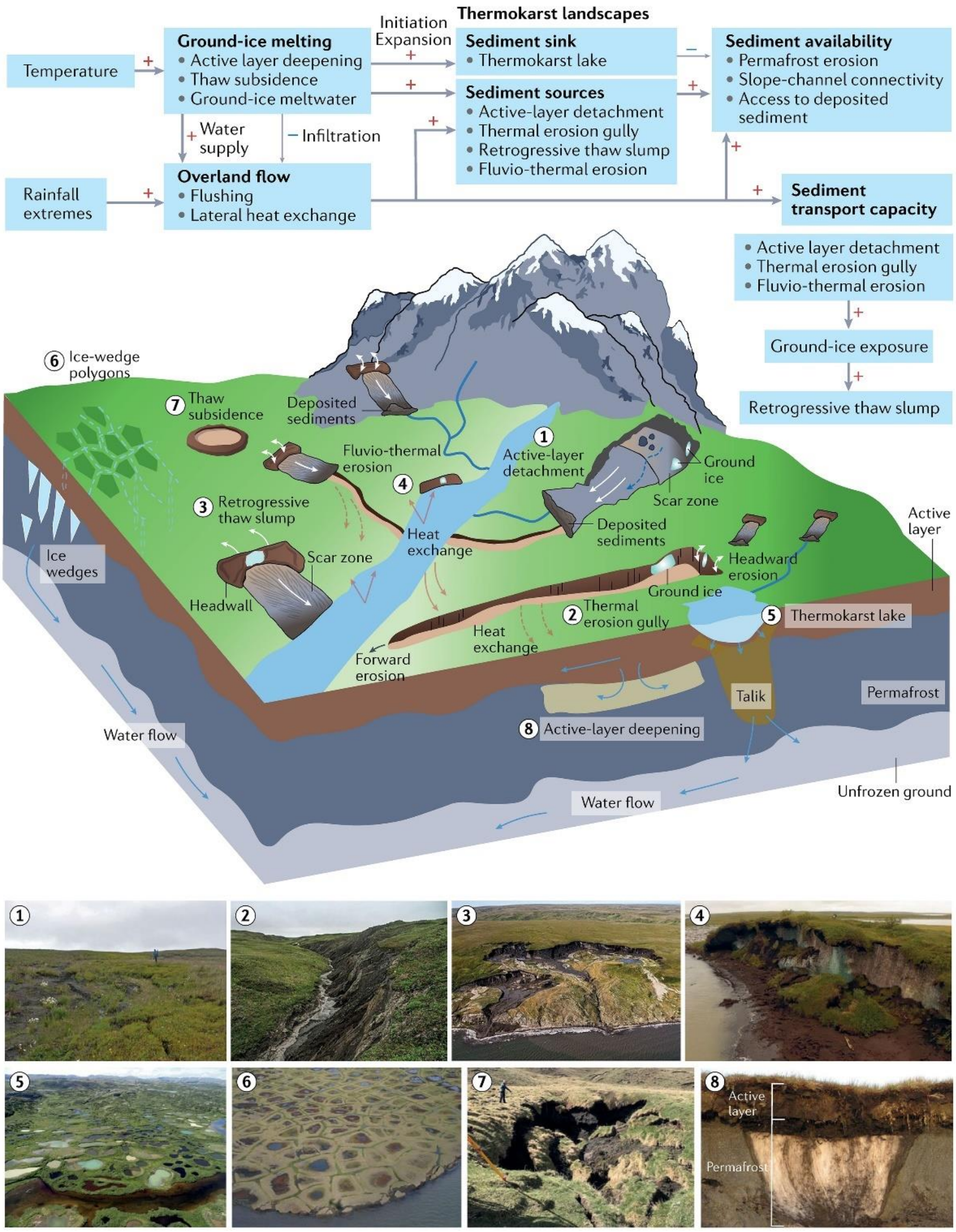

Figure 5. **Increased sediment fluxes due to modern climate change and cryosphere degradation. a** | 76 locations show increased sediment fluxes due to enhanced glacier melting permafrost disturbance, and combined glacier-permafrost impact. Among these, increased sediment fluxes at 57 locations (75%) are determined from decadal observations; increases at 10 locations from paired catchment comparisons (comparison of sediment fluxes from areas disturbed by glacier/permafrost-related processes with an undisturbed region); and 9 locations from typical year comparisons (sediment fluxes in a normal year vs. sediment fluxes in a disturbed year). Erosion rates along Arctic permafrost coasts are sourced from ref.[33], with accelerated coastal erosion rates observed in 18 locations (details in Supplementary Tables 1 and 2). Magnitudes of Greenland delta progradation from the 1940s to 2010s are sourced from ref.[4]. Sub-panels for region 5 and the Andes have been reprojected to the Equal Earth map projection to provide more intuitive visualization. **b** | Accelerated increases in annual suspended sediment flux (Qs, as percentage) and temperature anomalies in HMA over 1960-2017[1]. Shaded areas denote standard errors. Trends of Qs and temperature anomalies are fitted separately for 1960–1995 and 1995–2017 (grey dashed lines). **c** | Intensified erosion rates along Arctic permafrost coasts: Beaufort Sea coast, Alaska[72,183], Herschel Island coast, northern Canada[163], and Barents Sea coast, northeastern Russia[182]. **d** | Expanded Greenland delta area from the 1940s to 2010s[4]. Grey dots represent individual deltas; central horizontal black lines represent median values. The change in mean delta size of each period is shown as the red line.

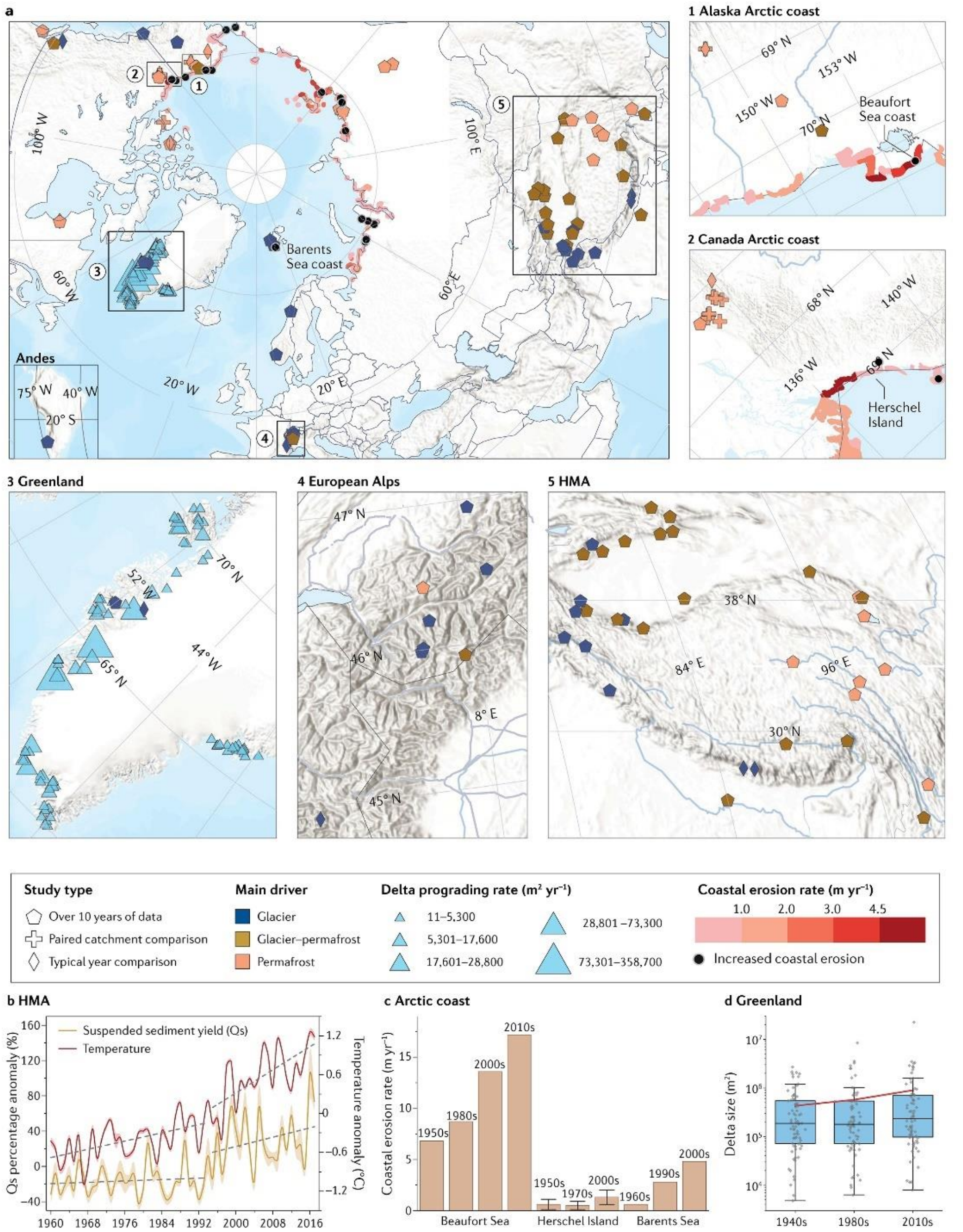

Figure 6. **Changes in basin-scale sediment source-to-sink processes in response to climate change and human activities.** The overall terrestrial sediment flux can be increased by sediment mobilization from retreated glaciers and thermokarst landscapes but decreased by the formation of natural and anthropogenic sediment sinks, with the net effect varying spatially. **a** | Present-day sediment source-to-sink processes. **b** | Sediment source-to-sink processes in a warmer future with intensified human activities. Brown arrows shown for both scenarios represent sediment fluxes of different magnitudes, with dash-dot, dashed, and solid lines representing low, medium, and high-sediment fluxes, respectively. Thick solid arrows denote increased sediment flux. Vegetation change (for example, reforestation, deforestation, and vegetation succession in proglacial areas) add uncertainties in estimating future changes in sediment yield.

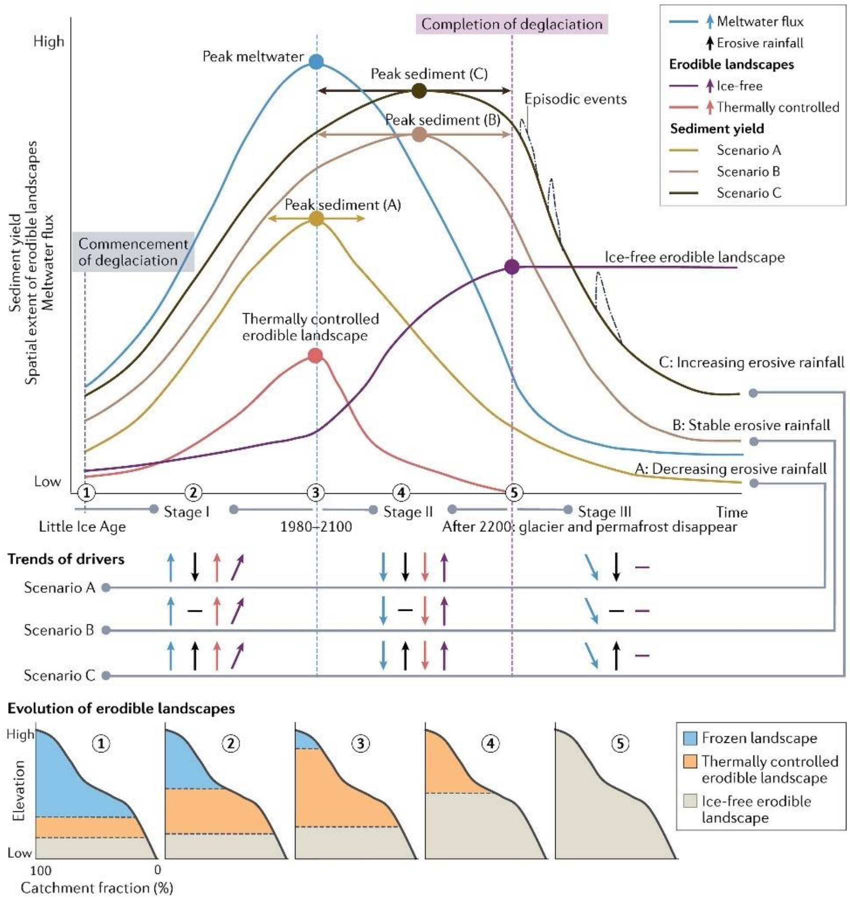

Figure 7| Peak sediment and transport regime changes.

Sediment transport regimes shift under a warming climate, in three stages. Stage I: thermally-controlled; stage II: thermally-and-precipitation-controlled; and stage III: precipitation-controlled, where pluvial processes, such as extreme rainfall and flooding, dominate. The timing of peak meltwater is inferred from a global-scale assessment of glacierized basins[11]; wherein the timing of completion of deglaciation is inferred from regional projections of cryosphere degradation[189-191]. The concept of peak sediment[75,176] incorporates the constraints of thermally-controlled and ice-free erodible landscapes, meltwater flux, and various rainfall scenarios in the upper panel. The three brown curves represent sediment fluxes and the timing of peak sediment under different erosive rainfall scenarios: A (decreasing), B (stable), and C (increasing). The timing and potential time range of the peak sediment flux are marked by the solid circle and dashed arrows, respectively. The basin hypsometry shown in the bottom panel represents the evolution of erodible landscapes during deglaciation, with the ice-free area in brown, the area with active thermally-controlled erosion in pink, and the frozen area with less effective erosion in blue. This projection of future sediment yield ignores glacier re-advance during cooling periods, (dis-)connectivity changes, scale and threshold effects in sediment transport, the stabilization rate of deglaciated landscapes, and human interference; and refers to relatively large mountainous cryospheric basins (larger than 1000 km^2).

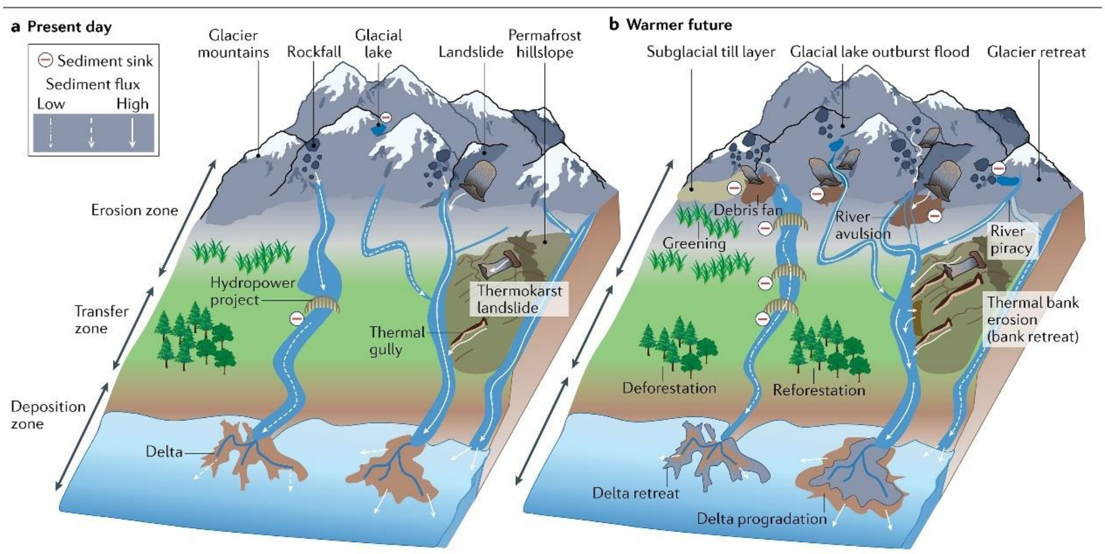

Glossary

CRYOSPHERE

The portion of Earth's surface where water exists in solid form, including glaciers, ice sheets, permafrost, snowpack, and river, lake and sea ice.

COLD REGIONS

High-altitude and/or high-latitude low-temperature environments, where hydrogeomorphic processes are influenced by glacier, permafrost, snow, or river, lake and sea ice.

CRYOSPHERIC BASINS

Basins where hydrological and geomorphic processes are influenced or even dominated by the cryosphere.

PEAK MELTWATER

The maximum of the meltwater in flux from the glacierized drainage basin; the meltwater flux initially increases with atmospheric warming and glacier melting, and then peaks, followed by a decline as glaciers shrink below a critical size.

PERMAFROST

Ground, consisting of ground ice, frozen sediments, biomass, and decomposed biomass, that remains at or below 0°C for at least 2 consecutive years.

YEDOMA PERMAFROST

A type of Pleistocene-age permafrost that contains a substantial amount of organic material (2% carbon by mass) and ground ice (ice content of 50-90% by volume)

ACTIVE LAYER

The top layer of soil or rock overlying the permafrost that experiences seasonal freeze (in winter) and thaw (in summer).

THERMOKARST LANDSCAPES

Landscapes with a variety of topographic depressions or collapses of unstable ground surface arising from ground-ice thawing, including active-layer detachment, thermal erosion gullies, retrogressive thaw slumps, and ice-rich riverbank collapse.

TALIK

A layer of soil or sediment in permafrost that remains unfrozen year-round, usually formed beneath surface water bodies.

GLACIAL LAKE OUTBURST FLOOD

A flood caused by the rapid draining of an ice-marginal or moraine-dammed glacial lake, or supraglacial lake.

BASAL SLIDING VELOCITY

The speed of slip of a glacier over its bed, which is facilitated by lubricating meltwater and limited by frictional resistance between the glacier sole and its bed.

PARAGLACIAL EROSION

Erosional processes directly conditioned by (de)glaciation, characterized by fluvial erosion and mass movements, including landslides, debris flows, and avalanches.

GLACIER EQUILIBRIUM LINE ALTITUDE

The elevation on a glacier where the accumulation of snow is balanced by ablation over a 1-year period.

PERIGLACIAL

Refer to cold and nonglacial landforms on the margin of past glaciers or geomorphic processes occurring in cold environments.

ICE-FREE ERODIBLE LANDSCAPES

Landscapes that are not covered by glaciers and contain no ground ice, where erosion is dominated by non-glacial or ice controlled–processes, including pluvial and fluvial processes.

THERMALLY-CONTROLLED ERODIBLE LANDSCAPES

Landscapes covered by glaciers and/or containing ground ice where erosion is dominated by glacial erosion and/or thermokarst erosion.